BRL MR 2599

BRL

AD

MEMORANDUM REPORT NO. 2599

COMPUTATIONAL PREDICTIONS OF SHOCK DIFFRACTION LOADING ON AN S-280 ELECTRICAL EQUIPMENT SHELTER

Richard E. Lottero

March 1976

Approved for public release; distribution unlimited.

USA BALLISTIC RESEARCH LABORATORIES
ABERDEEN PROVING GROUND, MARYLAND

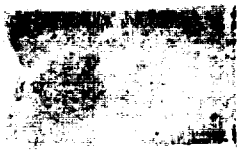

Destroy this report when it is no longer needed.
Do not return it to the originator.

Secondary distribution of this report by originating or sponsoring activity is prohibited.

Additional copies of this report may be obtained from the National Technical Information Service, U.S. Department of Commerce, Springfield, Virginia 22151.

The findings in this report are not to be construed as an official Department of the Army position, unless so designated by other authorized documents.

UNCLASSIFIED

SECURITY CLASSIFICATION OF THIS PAGE (When Data Entered)

REPORT DOCUMENTATION PAGE		READ INSTRUCTIONS BEFORE COMPLETING FORM
1. REPORT NUMBER BRL MEMORANDUM REPORT NO. 2599	2. GOVT ACCESSION NO.	3. RECIPIENT'S CATALOG NUMBER
4. TITLE (and Subtitle) COMPUTATIONAL PREDICTIONS OF SHOCK DIFFRACTION LOADING ON AN S-280 ELECTRICAL EQUIPMENT SHELTER		5. TYPE OF REPORT & PERIOD COVERED Memorandum 6. PERFORMING ORG. REPORT NUMBER
7. AUTHOR(s) Richard E. Lottero		8. CONTRACT OR GRANT NUMBER(s)
9. PERFORMING ORGANIZATION NAME AND ADDRESS USA Ballistic Research Laboratories Aberdeen Proving Ground, Maryland 21005		10. PROGRAM ELEMENT, PROJECT, TASK AREA & WORK UNIT NUMBERS 1W162118AH75
11. CONTROLLING OFFICE NAME AND ADDRESS US Army Materiel Development & Readiness Command 5001 Eisenhower Avenue Alexandria, Virginia 22304		12. REPORT DATE MARCH 1976 13. NUMBER OF PAGES 50
14. MONITORING AGENCY NAME & ADDRESS(if different from Controlling Office)		15. SECURITY CLASS. (of this report) UNCLASSIFIED 15a. DECLASSIFICATION/DOWNGRADING SCHEDULE

16. DISTRIBUTION STATEMENT (of this Report)

Approved for public release; distribution unlimited.

17. DISTRIBUTION STATEMENT (of the abstract entered in Block 20, if different from Report)

18. SUPPLEMENTARY NOTES

19. KEY WORDS (Continue on reverse side if necessary and identify by block number)

Transient Pressure Distributions
Shock Diffraction Loading
3-D Hydrodynamic Calculations
S-280 Electrical Equipment Shelter
Rectangular Parallelepiped Target

20. ABSTRACT (Continue on reverse side if necessary and identify by block number) ljc

The Los Alamos Scientific Laboratory, under contract to the BRL, utilized a three-dimensional, transient, hydrodynamics computer program, BAAL, developed at LASL, to compute the diffraction loading versus time caused by a one-dimensional 34.475 kPa (5.0 psi) overpressure steady shock wave striking an S-280 Electrical Equipment Shelter. The results of this computation have been placed on a magnetic tape at the BRL. Copies of this tape are available on request. The tape includes an alphanumeric introduction describing the data on the tape and overpressure - time histories for each computational flow

DD FORM 1 JAN 73 1473 EDITION OF 1 NOV 65 IS OBSOLETE UNCLASSIFIED (CONT'D)

SECURITY CLASSIFICATION OF THIS PAGE (When Data Entered)

(Item 20 Continued)

field cell that has a coincident face with either the shelter front, top, back, or side face. Also included on the tape is the time history of the resultant force due to overpressure and its effective point of application for each face. Although there are no direct experimental data available for comparison, the pressure - time histories generated appear to be quite good, with the possible exceptions of apparent pressure anomalies at the shelter edges where the flow undergoes a rapid 90 degree expansion, and the late - time pressures computed.

TABLE OF CONTENTS

LIST OF ILLUSTRATIONS

LIST OF ILLUSTRATIONS (CONT'D)

1. INTRODUCTION

The established methods[1] for estimating shock wave diffraction loading on simple structures do not differentiate between two- and three-dimensional geometries. A shock tube study performed at the BRL by Taylor[2] has indicated that significant differences exist in the shock wave diffraction loading - time histories for such structures.

Subsequent to Taylor's shock tube study was the completion of a study at the Los Alamos Scientific Laboratory involving the development by Pracht[3] of a three-dimensional, transient, viscous flow hydrodynamics computer program, BAAL, originally designed to calculate the late-time effects of atmospheric nuclear explosions. The program was modified to permit the inclusion of obstacles, allowing the computation of obstacle surface pressure - time histories for blast loading studies. To explore the possibility of using this hydrocode to determine diffraction loading on simple structures, the Ballistic Research Laboratories contracted with the Los Alamos Scientific Laboratory to perform a test calculation which could be compared with experimental data. Gentry et al[4] simulated one of Taylor's[2] three-dimensional shock tube experiments with a BAAL computer run. This experiment involved a one-dimensional, steady shock wave, of 34.475 kPa (5.0 psi) overpressure, striking a three-dimensional rectangular parallelepiped .2127 m wide, .1062 m high, and .0762 m deep, with the shock traveling in the direction of measure of the depth. Ambient conditions prior to shock arrival were a temperature of 288.16 Kelvin (15C), a pressure of 101.325 kPa (14.696 psi), and no flow. Since the BAAL computation was to be compared to the shock tube measurements, steady flow was specified behind the shock wave.

---

[1] *"Design of Structures to Resist the Effects of Atomic Weapons," U.S. Army Corps of Engineers, EM 1110-345-413 (1 July 1959).*

[2] *Taylor, W. J., "A Method for Predicting Blast Loads During the Diffraction Phase," The Shock and Vibration Bulletin, NR.42. Part 4 of 5, Shock and Vibration Center, Naval Research Laboratory, Washington, D. C., p. 135 (January 1972).*

[3] *Pracht, W. E., "Calculating Three-Dimensional Fluid Flows at All Speeds with an Eulerian-Lagrangian Computing Mesh," LA-UR-74-1137, University of California, Los Alamos Scientific Laboratory, Los Alamos, New Mexico (July 1974).*

[4] *Gentry, R. A., Stein, L. R., and Hirt, C. W., "Three Dimensional Computer Analysis of Shock Loads on a Simple Structure," BRL CR 219, U.S. Army Ballistic Research Laboratories, Aberdeen Proving Ground, MD (March 1975). AD# B003208L.*

The BAAL computer code has the general capability of solving the following system of differential equations in their integral form.

$$\frac{\partial \rho}{\partial t} + \frac{\partial \rho u_j}{\partial x_j} = 0 \ , \tag{1}$$

$$\frac{\partial \rho u_i}{\partial t} + \frac{\partial}{\partial x_j}\left(\rho u_i u_j - p_{ij}\right) = g_i \rho \ ^{*} \ , \tag{2}$$

where

$$p_{ij} = - p\delta_{ij} + \tfrac{1}{2} \lambda e_{kk} \delta_{ij} + \mu e_{ij} \ , \tag{3}$$

$$e_{ij} = \frac{\partial u_i}{\partial x_j} + \frac{\partial u_j}{\partial x_i} \ , \tag{4}$$

and

$$\frac{\partial \rho E}{\partial t} + \frac{\partial}{\partial x_j}\left(\rho u_j E - p_{ij} u_i - \mu B \frac{\partial I}{\partial x_j}\right) = \rho u_j g_j \ , \tag{5}$$

where

$$E = \tfrac{1}{2} u_i^2 + I \ . \tag{6}$$

The stress tensor is represented by p_{ij}, wherein p is the scalar pressure, and λ and μ are the viscosity coefficients. The term g_i represents the gravitational acceleration, which is neglected here; E is the specific total energy; I is the specific internal energy; δ_{ij} is the Kronecker delta. The heat conduction term in the energy equation is written as a spatial gradient in I, multiplied by viscosity μ and an input coefficient B.

The BAAL computations for the shock tube model calculation, and for the S-280 Electrical Equipment Shelter calculation reported here, were made using the above set of differential equations in their integral form, with one major modification. The Navier-Stokes equations, Eqs (2), (3),

---

* *For the calculations reported here, the Navier-Stokes equations have been replaced by the inviscid Euler equations, with the added feature of an artificial viscosity being introducted whenever the flow undergoes a deceleration.*

and (4), have been replaced by the inviscid Euler equations, with an artificial viscosity significantly larger than real viscosity being introduced for purposes of numerical stability in regions of high deceleration. The artificial viscosity computed under this criterion is manifested as a simple addition to the scalar pressure. No shearing stresses are calculated. Free slip flow is specified at all boundaries.

These simplifications to the Navier-Stokes equations were deemed expedient because of the large cell sizes dictated by practical computer time and storage limitations. The active computational flow field grid for the shelter calculation consists of 6750 cells, not counting boundary cells, but including those cells occupied by the ½ width shelter. The cells were of varying sizes, with the smallest cell dimension at the shelter boundary being approximately 0.14 m. This smallest cell dimension is estimated to be several times larger than any boundary layer that could develop on the shelter during the shock diffraction phase. The use of the Navier-Stokes equations with a no-slip boundary condition would have resulted in unrealistically large computed boundary layers. A similar situation exists for the shock tube model calculation.

Both computations involved a relatively weak 34.475 kPa (5.0 psi) overpressure shock wave in air. Hence, the polytropic equation of state

$$p = \rho I \ (\gamma - 1) \tag{7}$$

with

$$\gamma = 1.4$$

was used to calculate the scalar pressure.

Comparisons between the computed and experimentally measured pressure - time histories at three points each on the front and back faces of the model are made in Reference 4. Agreement is excellent for all three points on the front face of the model. The theoretical peak reflected overpressure is 78.54 kPa (11.39 psi). The peak experimentally measured overpressure, averaged over these three points, is 75.8 kPa (11.0 psi), approximately 3% below the theoretical peak overpressure. This excellent agreement of the experimentally measured peak with the theoretical peak implies that the experiment yielded accurate data and is a valid standard against which the calculated values may be compared. Using this experimental standard, the following comparisons may be made.

The peak overpressure calculated using the BAAL computer code is 75.1 kPa (10.9 psi), occurring at approximately 50 μs after the theoretical arrival of the shock wave at the front face, and equal to the experimental overpressure for that time. At 200 μs, the computed average overpressure is 1% higher than the experimentally measured average overpressure, 6% lower at 400 μs, 3% higher at 600 μs, and 3% higher at 800 μs.

Agreement between the experimentally measured average overpressure and the calculated average overpressure for the three points on the back face is good, but not as good as that for the front face. For purposes of this comparison, zero time is defined as that time at which the theoretical shock wave reaches the plane of the back surface of the shelter. The computed average overpressure for the three points on the back surface is 21% lower than the experimentally measured overpressure at 100 μs after this redefined reference time, 6% lower at 200 μs, equal at 300 μs, 15% higher at 400 μs, 4% higher at 500 μs, and 6% higher at 600 μs. Shortly thereafter, it was determined that reflected signals were returning from the mesh boundaries, causing spurious pressure rises, and the computation was stopped. There were no experimental measurements made on the top or side faces.

II. S-280 ELECTRICAL EQUIPMENT SHELTER CALCULATION

The agreement between Taylor's[2] shock tube experiment and the BAAL computer simulation led to the running of a second problem with BAAL, also under contract to the BRL. The results of this second computation are reported here. The three-dimensional rectangular parallelepiped for this computation is a full scale S-280 Electrical Equipment Shelter as shown in Figure 1. The shelter dimensions are width X = 3.6200 m, depth Y = 2.1720 m, and height Z = 2.1085 m. The shelter is sitting on the ground with its largest face, defined here as the front face, oriented so that it is normal to the velocity vector of the oncoming one-dimensional shock wave. A one-half width shelter was used in the computation, taking advantage of the existing plane of symmetry. The active computational flow field consisted of 6750 cells, not counting boundary cells but including those cells occupied by the one-half width S-280 shelter. The one-half width S-280 shelter occupies 7 cells in the X direction, 9 cells in the Y direction, and 7 cells in the Z direction. The cells are of variable size. The upstream end of the computing mesh is 6.27 m removed from the front face of the shelter, and the downstream end of the computing mesh is 12.16 m removed from the back face of the shelter. The top of the computing mesh is 6.34 m removed from the top face of the shelter. One side of the computing mesh, the reflective plane, is coincident with the symmetry plane down the depth of the shelter, and the other side of the computing mesh is 6.20 m removed from the side of the shelter. The computation was started with the shock at the front face, as was the computation for the previously discussed shock tube model.

Surface loadings for a whole shelter are reported here. Initial conditions and shock overpressure are the same as for the calculation involving the smaller shock tube model. The shock tube model does not scale directly to the S-280 shelter. As before, steady flow is specified behind the shock, simulating zero decay blast wave conditions for maximum diffraction loading for that shock overpressure. The time required for the shock to travel the depth of the S-280 shelter, hereafter referred to as the shock traversal time, is slightly over 5.6×10^{-3} s.

The data tape, available from the BRL on request, includes overpressure - time histories for each computational flow field cell that has one of its faces coincident with the front, top, back, or side face of the S-280 shelter. The tape also includes a time-history of the resultant force due to overpressure for each entire face, and the effective point of application for that force. Other flow field data are not presently available. Although the data are presented as if those overpressures were computed directly on the shelter surface, they are actually computed at the respective flow field cell centers, which are displaced from the shelter surface by one half of the cell dimension in the I, J, or K direction. Figures 2a, 2b, and 2c show the S-280 shelter surface grid spacings, and the cell centers at which surface overpressure - time histories are computed and tabulated.

III. DISCUSSION

The pressure - time histories for the surfaces of the S-280 shelter as calculated by the BAAL program appear to be quite good in general, although there are no direct experimental data available for comparison. There is, however, one apparent anomaly that appears consistently throughout the pressure - time histories of the BAAL computations for both the three-dimensional shock tube model and the S-280 shelter. Around those model or shelter corners where the flow undergoes a 90 degree expansion, the BAAL program computes unexplained, often sharp, pressure increases seen when comparing the overpressure for the next-to-last flow field cell at the model surface to that for the last flow field cell at the surface prior to the corner. Specifically, the affected rows and columns are the top row of cells on the front face, the last column of cells on the front face, the last row of cells on the top face, and the last column of cells on the side face. These pressure increases are on the order of 10 to 30 percent, using the calculated overpressure for the next-to-last cell in any given case as the basis for comparison. Since it can reasonably be expected that in general there should be a further drop in pressure at these corners rather than a rise, the actual overpressure at these corners may be significantly less than the calculated values. Figures 3a through 3h show a sequential pressure - time history for the fourth row of cells up the side face (the cell centers being at approximately 2/3 of the shelter height), a typical illustration of this anomaly. Shock smearing in the relatively large computational flow field cells is also readily evident.

The cause of this pressure increase has not yet been established, nor has a correction factor been established for modifying these corner effects if, as suspected, they are caused by difficulties in the computational algorithm being utilized. The overpressure data available on magnetic tape is stored as it was presented to the BRL by LASL, with no modifications except for a simple change of units. Resultant force due to overpressure and the effective point of application for each entire shelter face were calculated at the BRL using the overpressure data. These were added to the data tape for the user's convenience.

Figure 4a shows the time history of the resultant force due to overpressure on the front face of the shelter, obtained by making a cell area weighted integration of the overpressure on the front face at each point in time,

$$F = \sum_{i=1}^{N} A_i P_i \quad . \tag{8}$$

Here A_i is the cell area, P_i is the overpressure associated with that cell, and N is the number of cells on the front face. Figure 4b shows the Z location of the effective point of application of the resultant force due to overpressure on the front face, obtained by summing cell area weighted moments,

$$Z_{eff} = \frac{\sum_{i=1}^{N} A_i P_i Z_i}{\sum_{i=1}^{N} A_i P_i} \quad . \tag{9}$$

Here Z_i is the measure of length from the ground to the i^{th} cell center, and the other variables are as defined above. It was expected that Figure 4b would show more of a bias of Z_{eff} toward the ground level at an earlier time than is indicated, since the high pressure should persist longer there. This apparent lack of bias may be due to the high pressure anomaly in the top row of cells. Figures 5a and 5b, 6a and 6b, and 7a, 7b, and 7c show similar data for the top, back, and side faces, respectively.

Figure 8a shows the average overpressure - time history for both the front and back faces. The average overpressure for a given face is calculated by

$$P = \frac{\sum_{i=1}^{N} A_i P_i}{\sum_{i=1}^{N} A_i} \quad . \tag{10}$$

The closest approach of the two curves to one another occurs at approximately 1.9×10^{-2}s (approximately 3.4 shock traversal times) after shock arrival at the front face. At this time the average overpressures are quite close to the incident shock overpressure of 34.475 kPa, with the front face approximately 11% higher and the back face approximately 4% lower. The front face average overpressure then rises with time during the rest of the computation, indicating an over-relieving of the reflected overpressure, occurring around the 1.9×10^{-2}s mark. This apparent over-relief and subsequent pressure rise has also been observed experimentally.[2] Figure 8b shows the average overpressure for both the top and side faces versus time. These curves are nearly identical up to approximately 6.0×10^{-3}s, roughly the shock traversal time. At this time, both curves peak at approximately the incident shock overpressure. This is to be expected, as this represents a loading of the top and side faces equal to the incident shock overpressure as the shock travels down the shelter. Thereafter, the average overpressures for the top and side faces oscillate slightly out of phase with one another just below the incident shock overpressure. These oscillations are probably due to transient waves in the computational flow field.

IV. CONCLUDING REMARKS

Comparison of the overpressure - time histories measured by Taylor[2] with those generated by Gentry et al[4] using the BAAL computer program indicates that the possibility now exists for supplementing experimental data on simple three-dimensional shapes with computational simulations of actual flow conditions, if it is done carefully and with a full understanding of the limitations of the computational program being used. The report by Gentry et al[4] concerning the shock tube model computation indicates excellent agreement between the computed and experimental overpressure - time histories for the front face. The peak reflected overpressure computed on the front face of S-280 shelter is essentially equal to the theoretical peak reflected overpressure. Taken together, these observations imply that the BAAL computation for the front face loading of the S-280 shelter is an accurate simulation of the loading to be expected under actual conditions. As noted earlier, the computed overpressure - time histories of the top and side faces of the S-280 shelter agree well with expectations on theoretical grounds, and thus may also be regarded as accurate. The only obvious discrepancies in the overpressure - time histories for the front, top, and side faces are the pressure anomalies at those corners where the flow undergoes a 90 degree expansion.

As indicated previously in the report by Gentry et al[4], the BAAL computation for the overpressure - time history on the back face of the shock tube model did not agree as well with experiment as did that for the front face of the model, particularly at late time near the edge of the model. This is not surprising. For a target of this general shape

with this type of loading, it is to be expected that viscous effects will be most pronounced on the back surface. Because of practical computer time and storage limitations, it was necessary to use a computational grid with relatively large cell sizes. This was also the case for the S-280 shelter computation. For both computations the smallest cell dimensions were significantly larger than any boundary layers that would be generated under actual flow conditions. There was also considerable numerical diffusion of the shock wave in these necessarily large grids. As a consequence, the addition of the viscous terms in the Navier-Stokes equations would add only complexity and additional computational time to the computer solution, but not accuracy. For these reasons, the Navier-Stokes equations were replaced by the inviscid Euler equations, using artificial viscosity for numerical stability. Since the computation for the shock tube model did not simulate viscous effects, it is understandable that the computed pressure - time history for the back face did not agree as well with experiment as did that for the front face. These difficulties are not unique to BAAL, but rather are common to all simulations of high Reynolds number flow.

For the same reasons, it can be expected that the computational predictions for the pressure - time history on the back face of the S-280 shelter will also be found at variance with experimental measurements, once they are made. Nonetheless, the pressure - time histories presented here, as computed using the BAAL computer program, represent the best estimate to date of the shock diffraction loadingon an S-280 Electrical Equipment Shelter.

V. ACKNOWLEDGEMENTS

Thanks are extended to R. A. Gentry, L. R. Stern, and C. W. Hirt of the Los Alamos Scientific Laboratory for their cooperation in performing these computations for the BRL. The assistance of Mr. John Wortman in generating the data tapes and plots has been most appreciated. Thanks are also extended to Mr. Noel Ethridge for his advice and contributions.

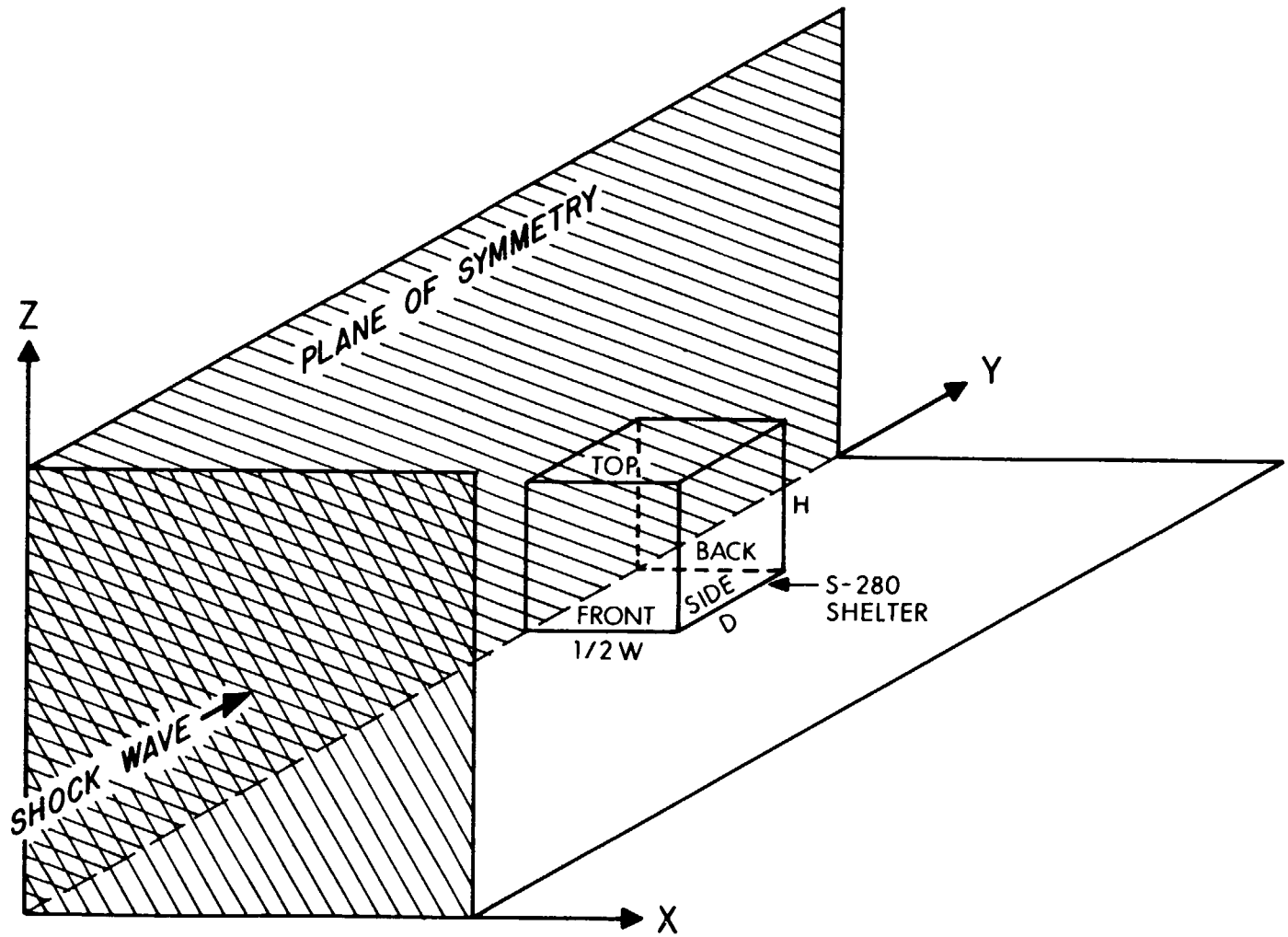

Figure 1. S-280 Electrical Equipment Shelter in the computational flow field.

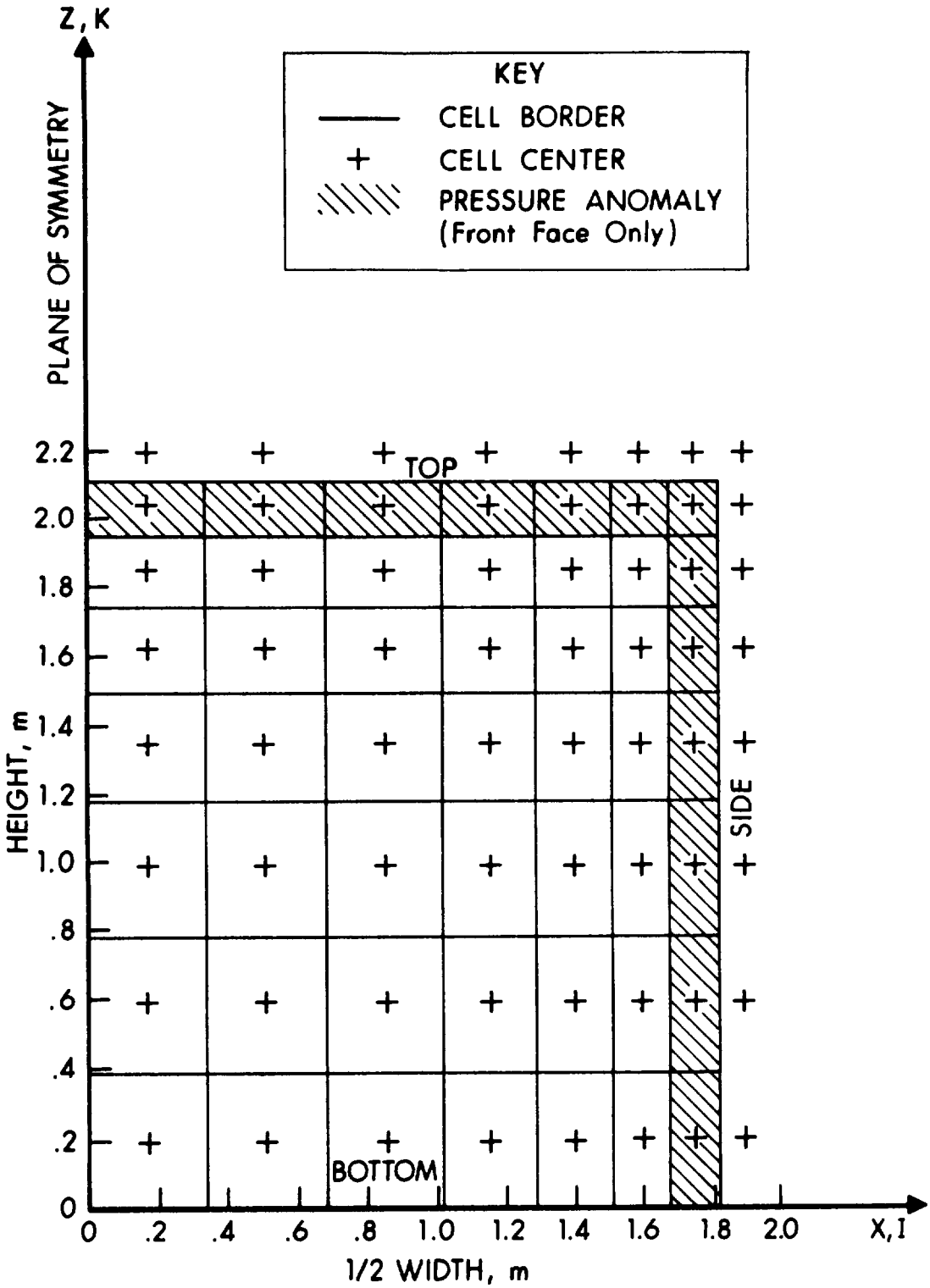

Figure 2a. Computational grid, front face. (Identical back face.)

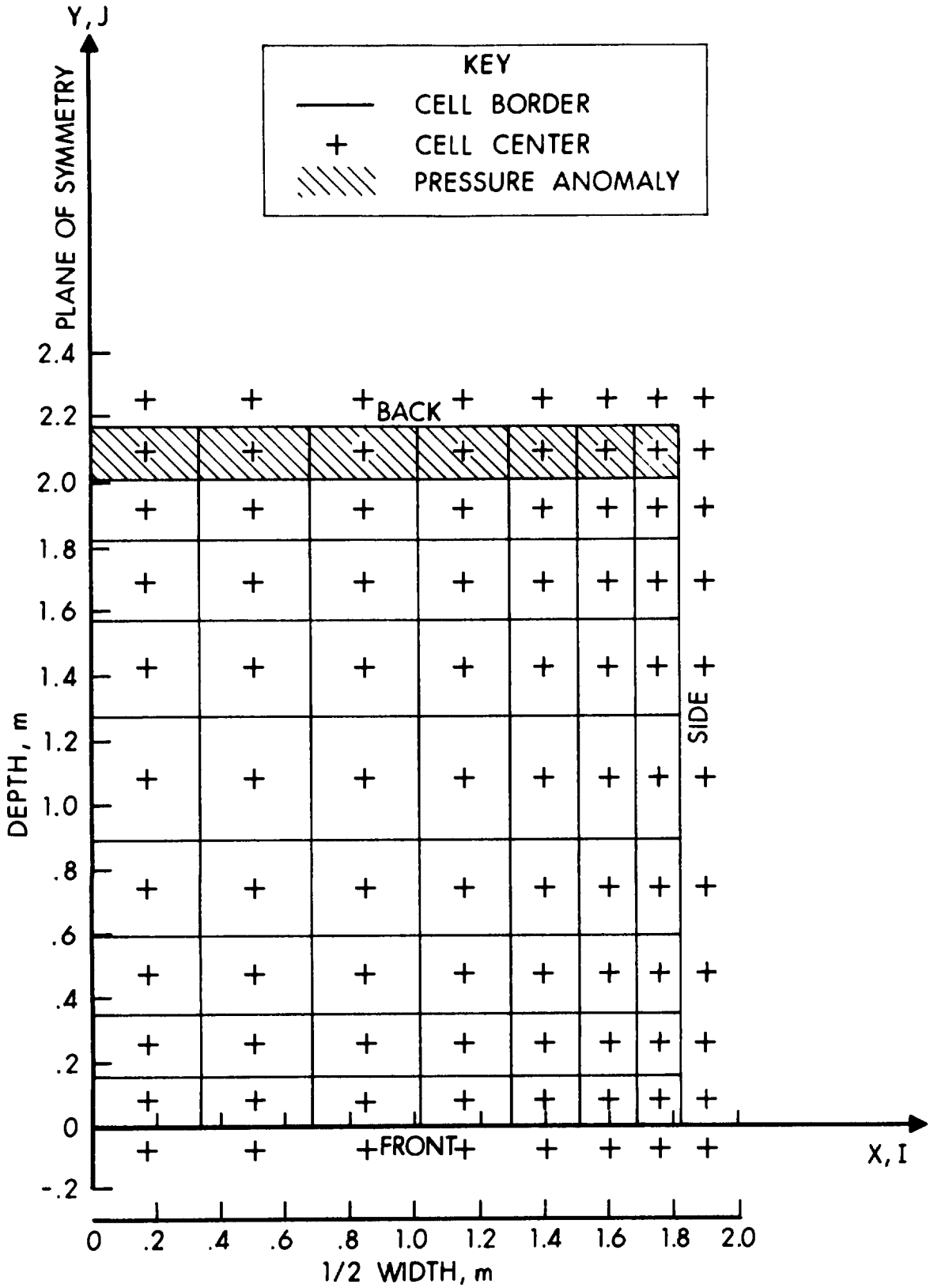

Figure 2b. Computational grid, top face.

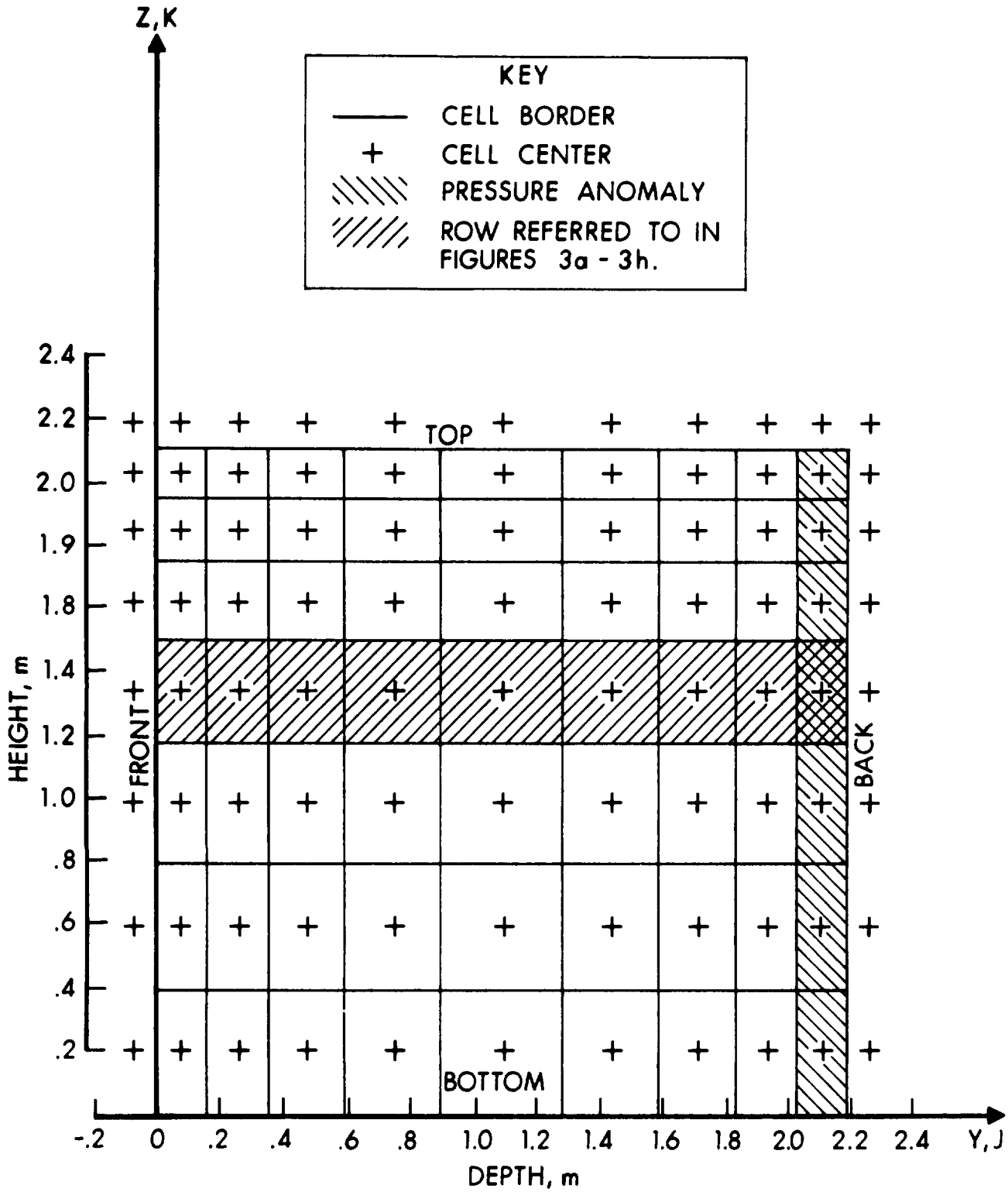

Figure 2c. Computational grid, side face.

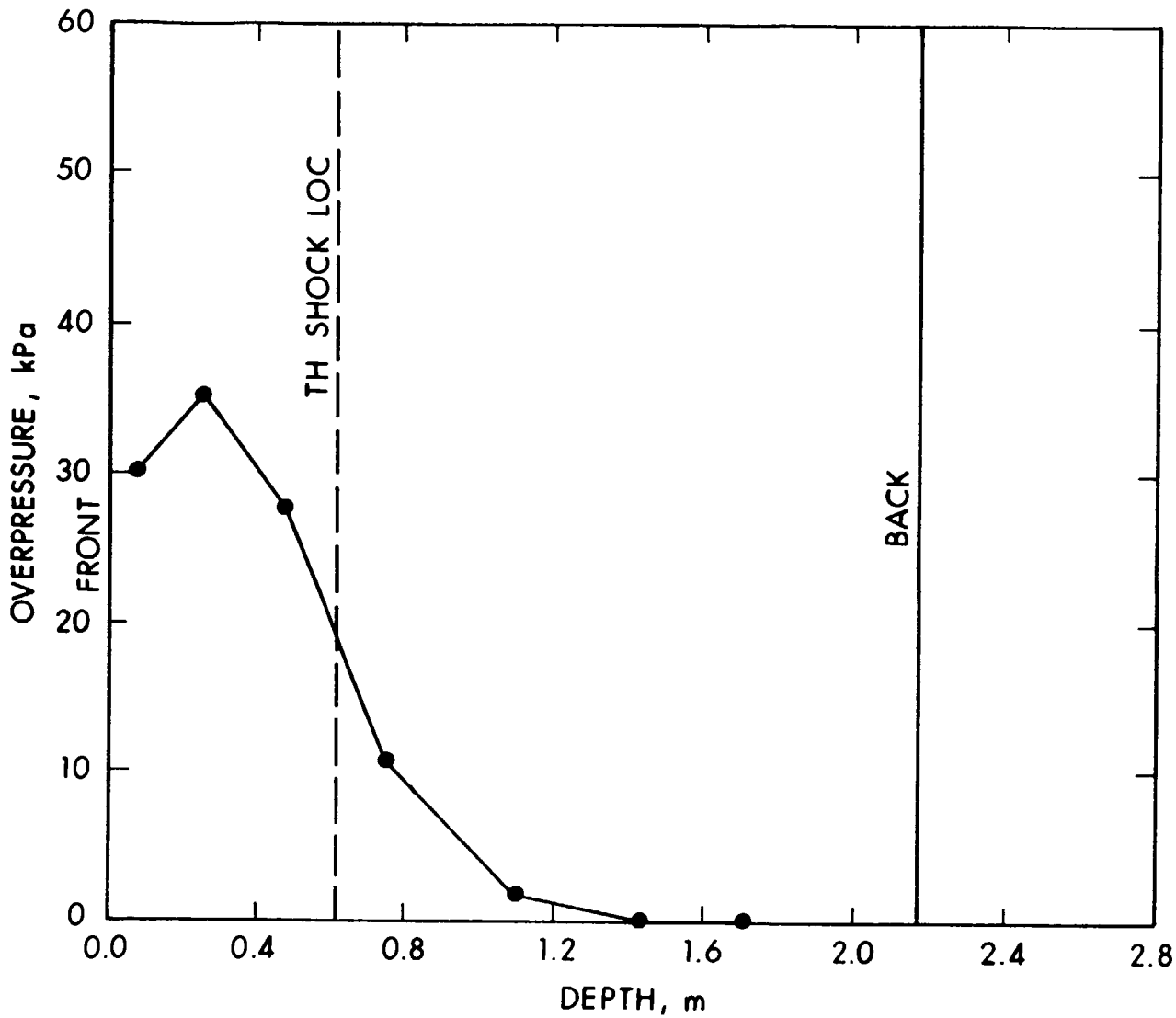

Figure 3a. Overpressure along the fourth row up the side face of the S-280 shelter. Time = 1.57×10^{-3} s after shock arrival at the front face.

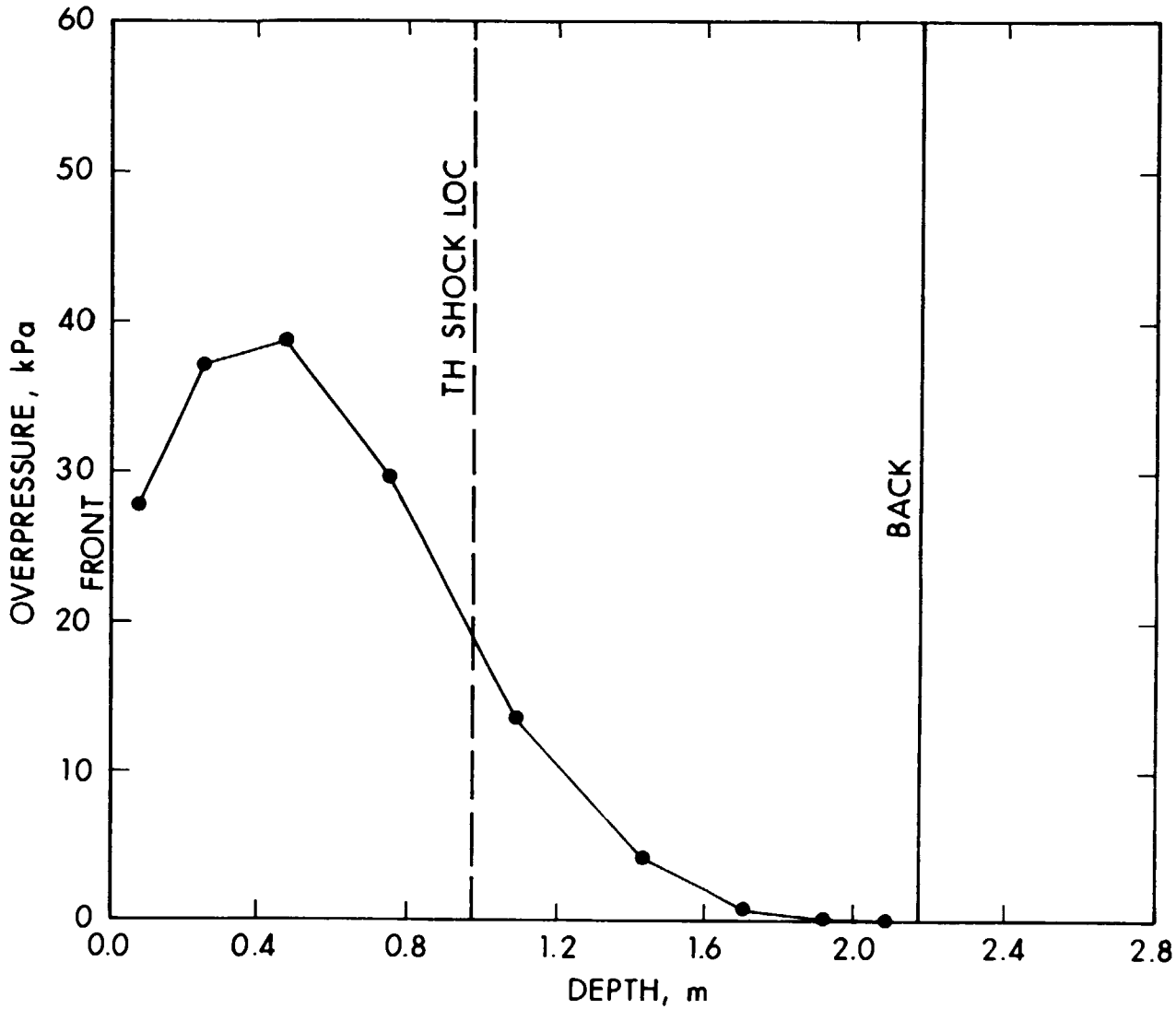

Figure 3b. Overpressure along the fourth row up the side face of the S-280 shelter. Time = 2.51×10^{-3} s after shock arrival at the front face.

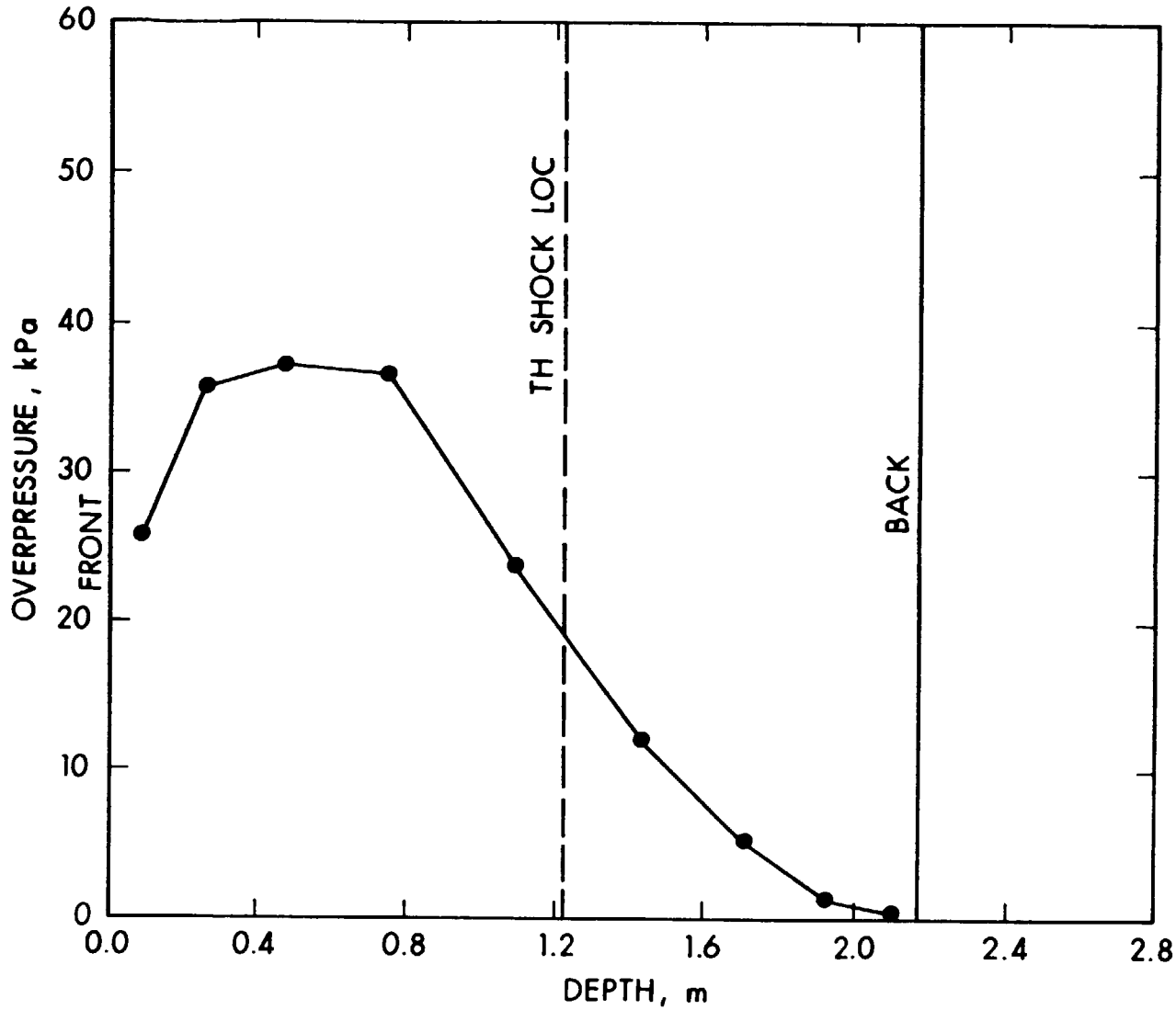

Figure 3c. Overpressure along the fourth row up the side face of the S-280 shelter. Time = 3.14×10^{-3} s after shock arrival at the front face.

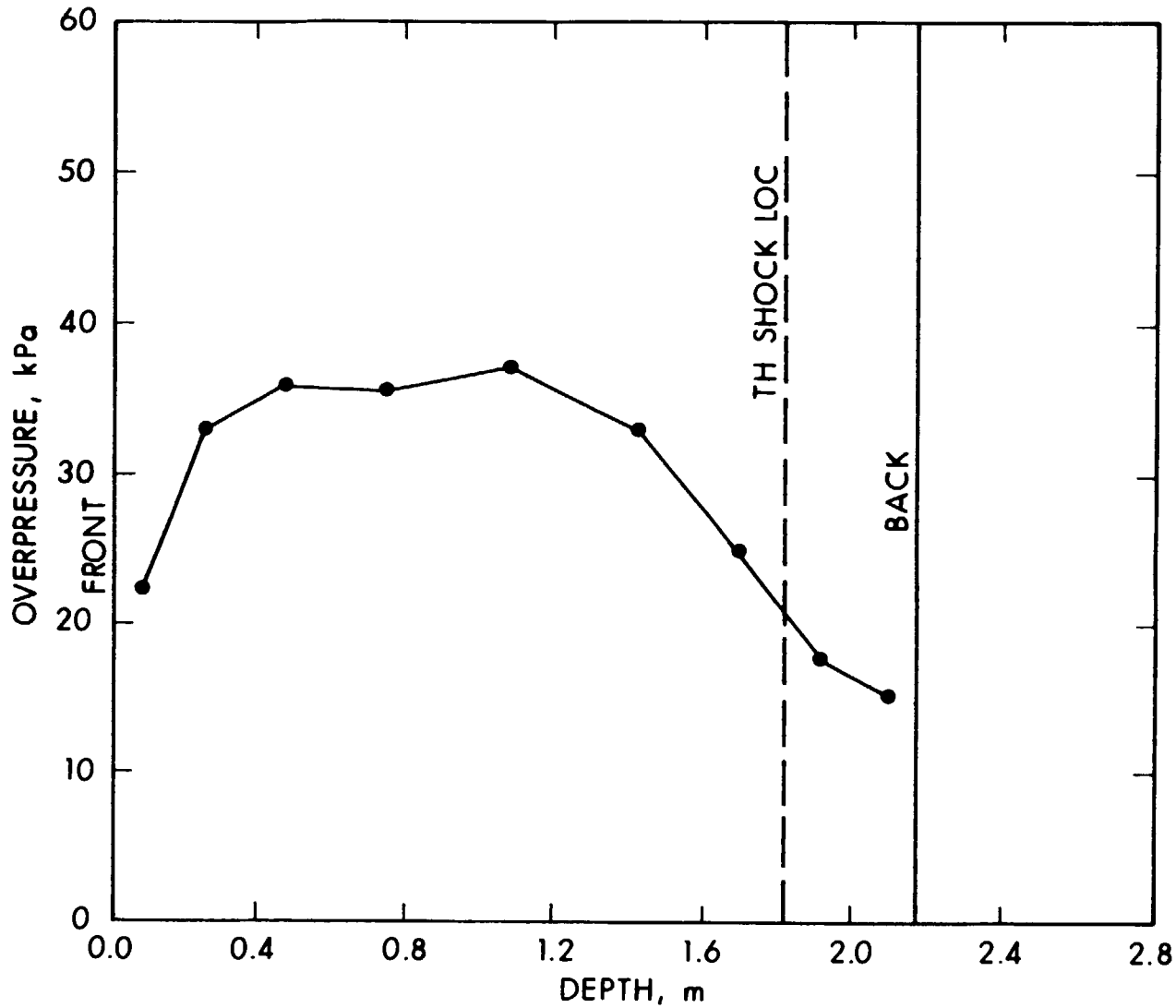

Figure 3d. Overpressure along the fourth row up the side face of the S-280 shelter. Time = 4.71×10^{-3} s after shock arrival at the front face.

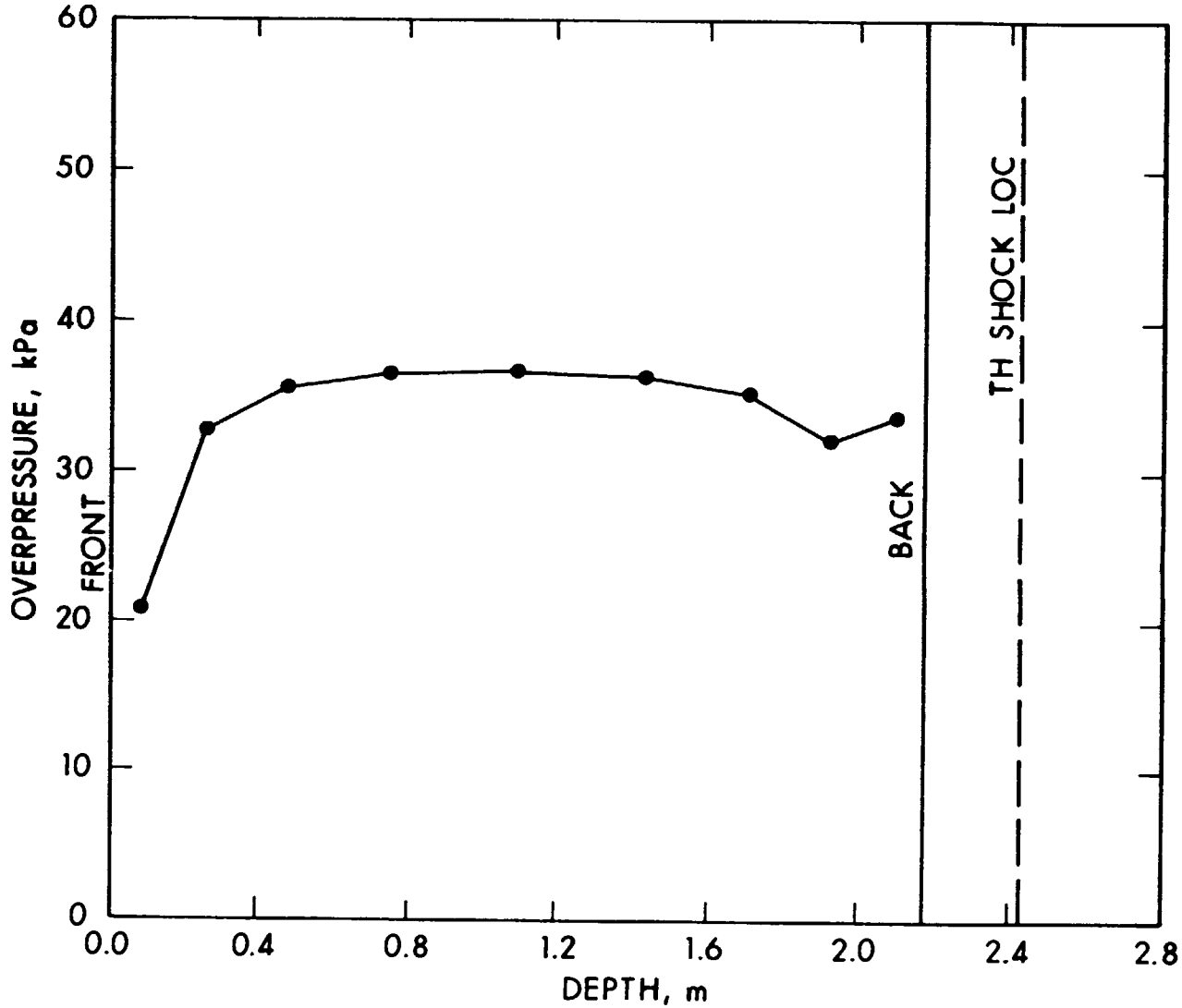

Figure 3e. Overpressure along the fourth row up the side face of the S-280 shelter. Time = 6.29×10^{-3} s after shock arrival at the front face.

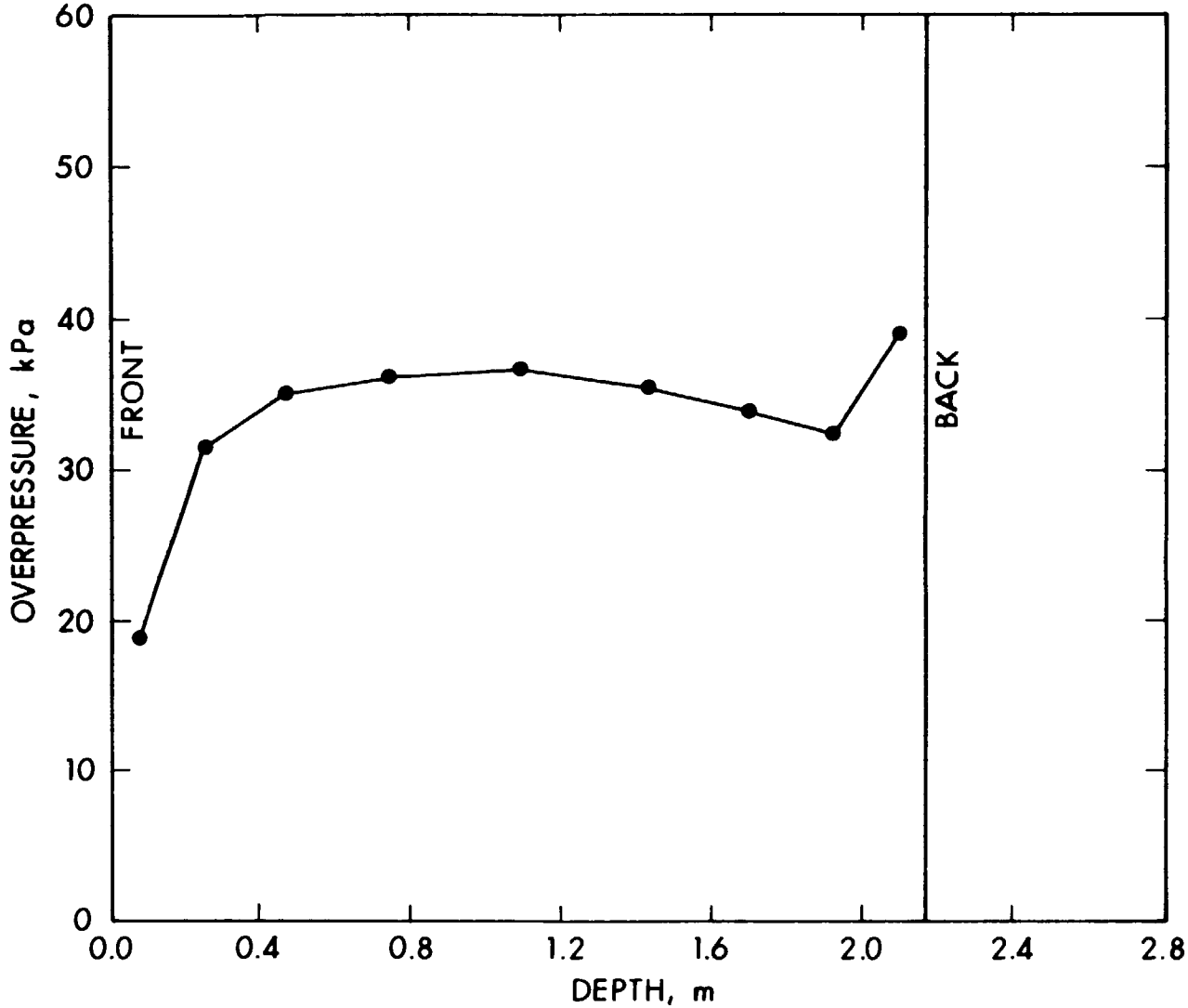

Figure 3f. Overpressure along the fourth row up the side face of the S-280 shelter. Time = 7.86×10^{-3} s after shock arrival at the front face.

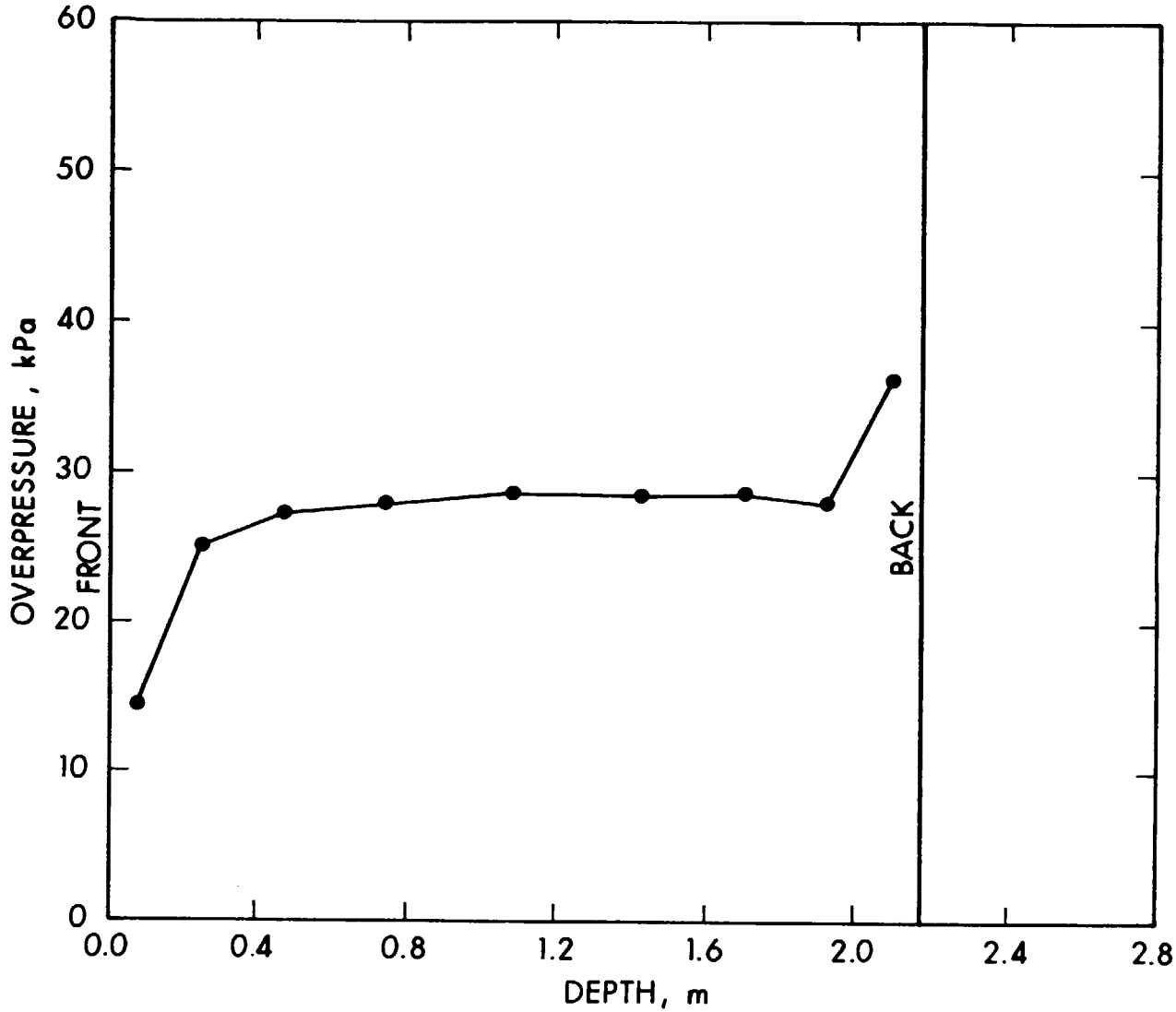

Figure 3g. Overpressure along the fourth row up the side face of the S-280 shelter. Time = 15.71 x 10^{-3} s after shock arrival at the front face.

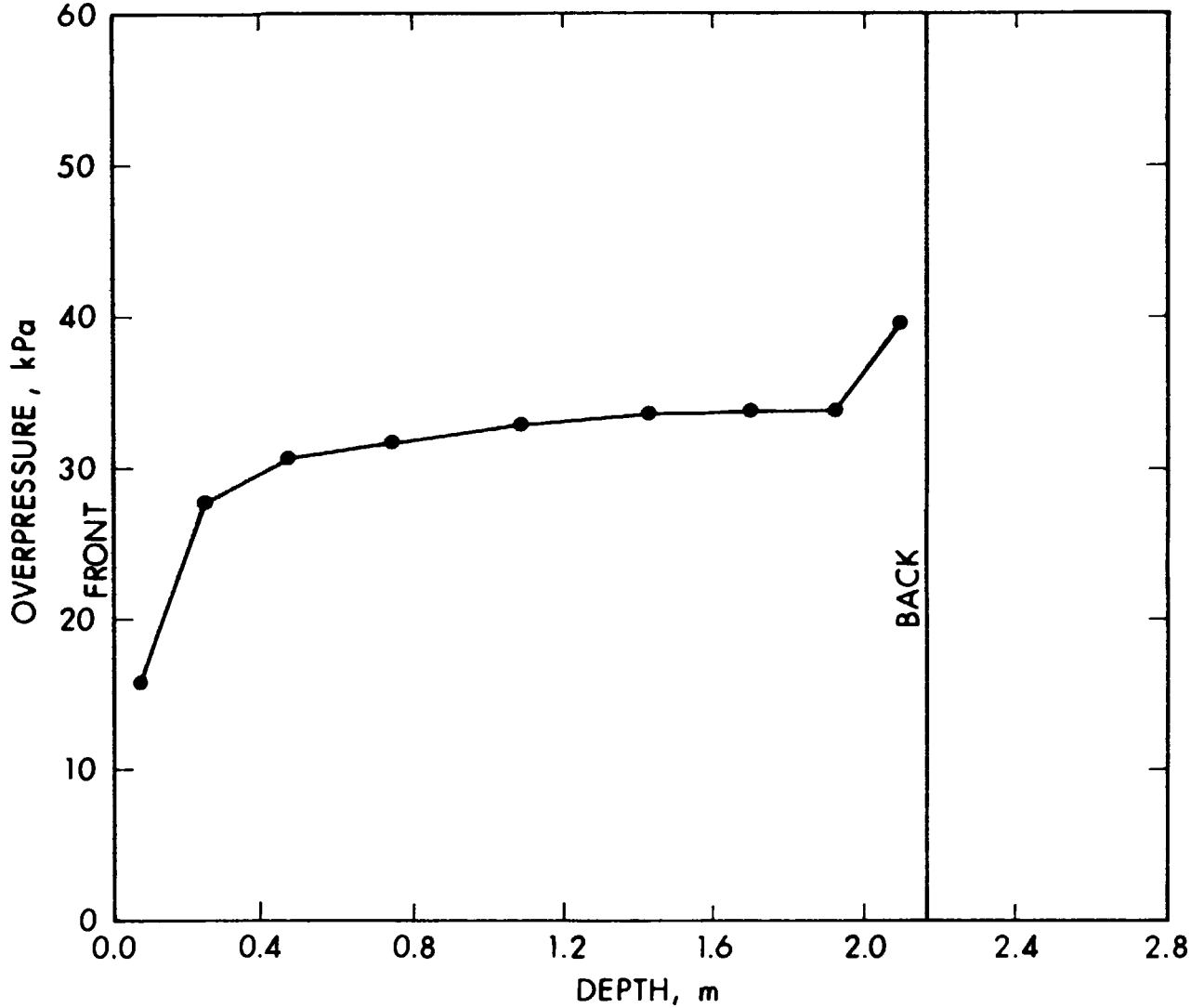

Figure 3h. Overpressure along the fourth row up the side face of the S-280 shelter. Time = 33.63 x 10^{-3} s after shock arrival at the front face.

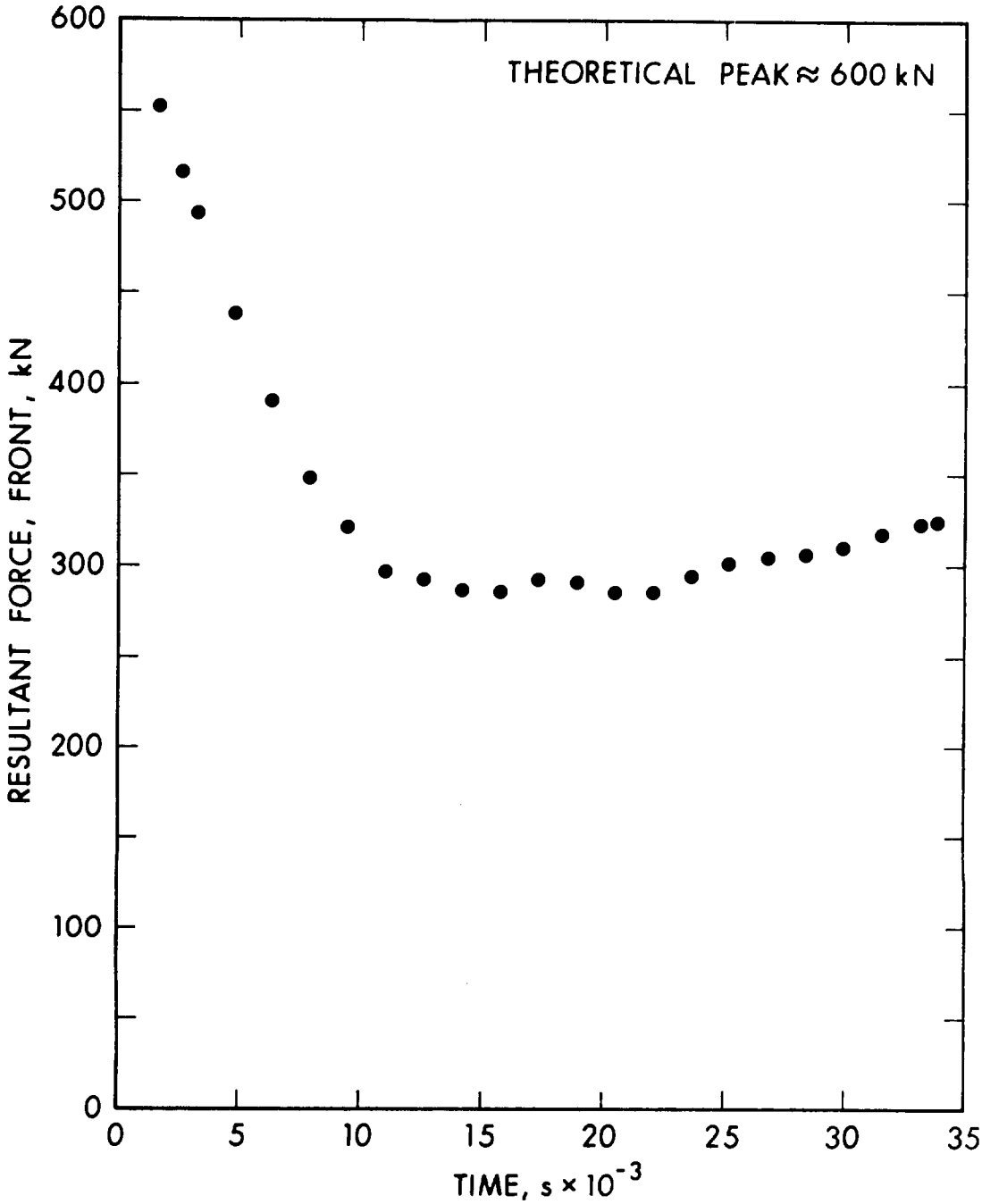

Figure 4a. The resultant force due to overpressure versus time for the front face.

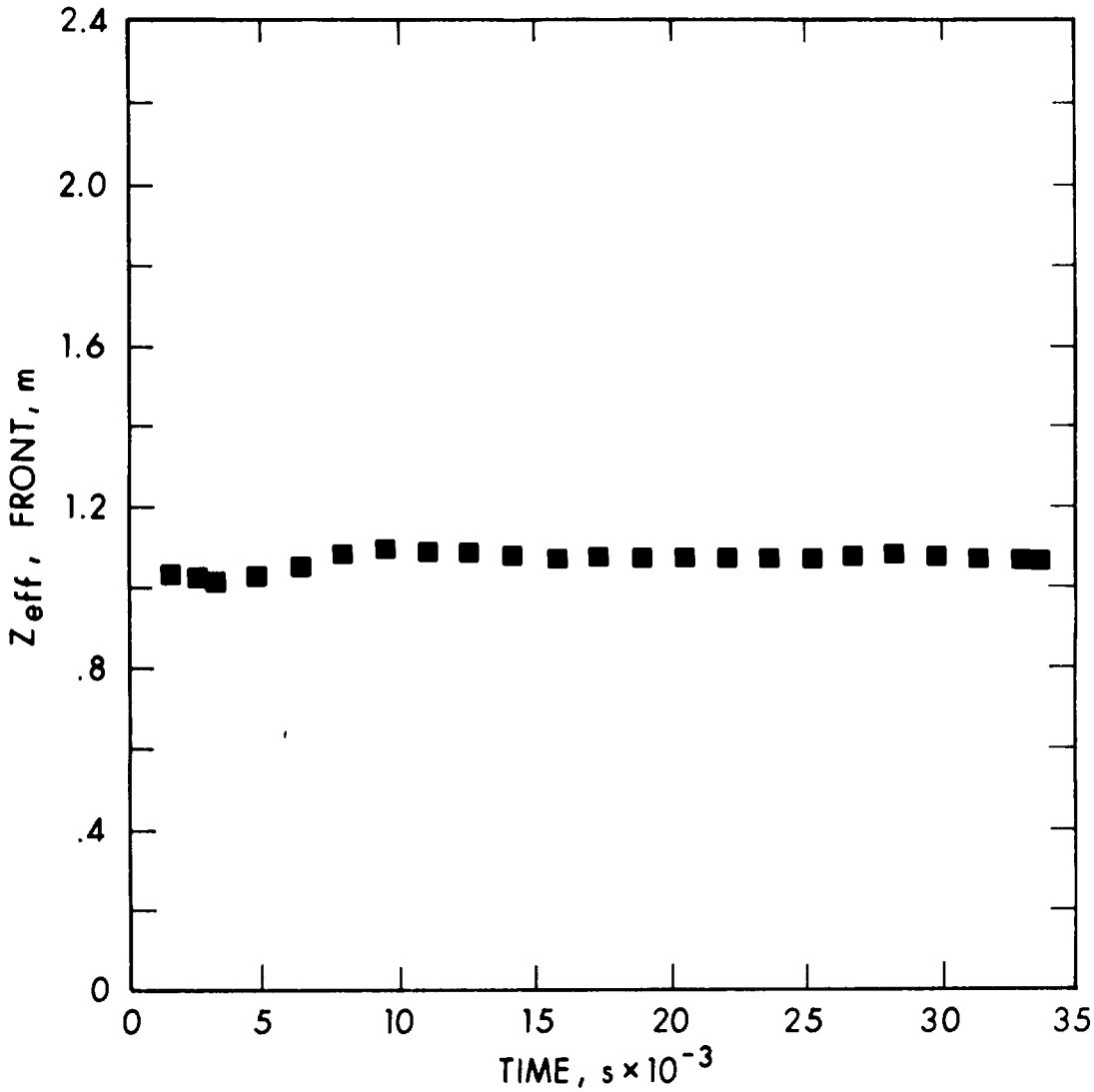

Figure 4b. The Z location of the effective point of application of the resultant force due to overpressure versus time for the front face.

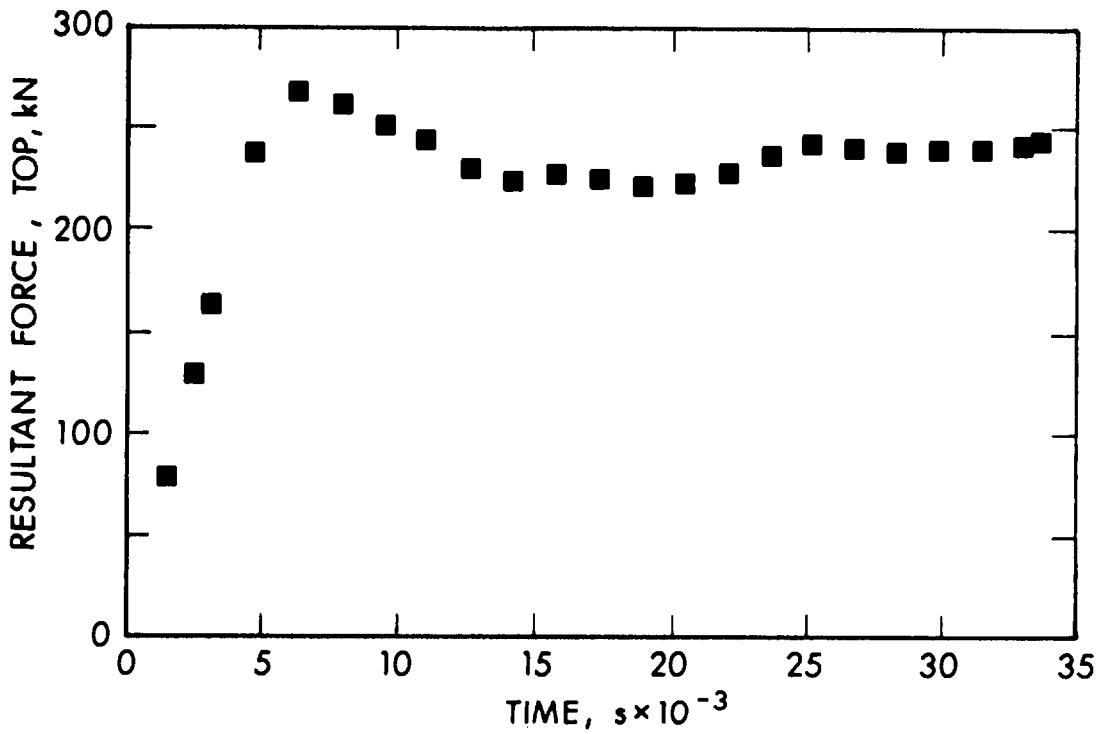

Figure 5a. The resultant force due to overpressure versus time for the top face.

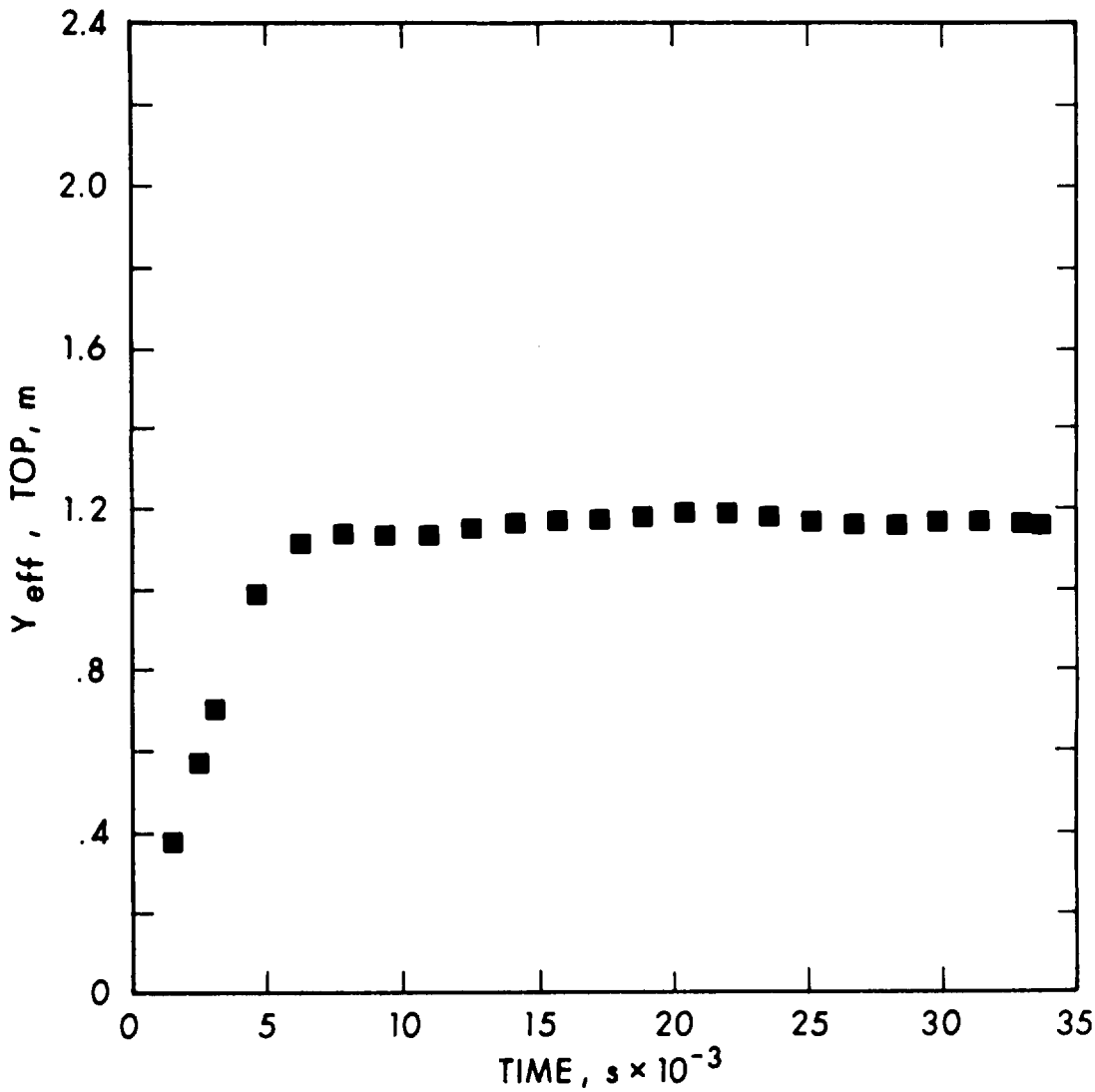

Figure 5b. The Y location of the effective point of application of the resultant force due to overpressure versus time for the top face.

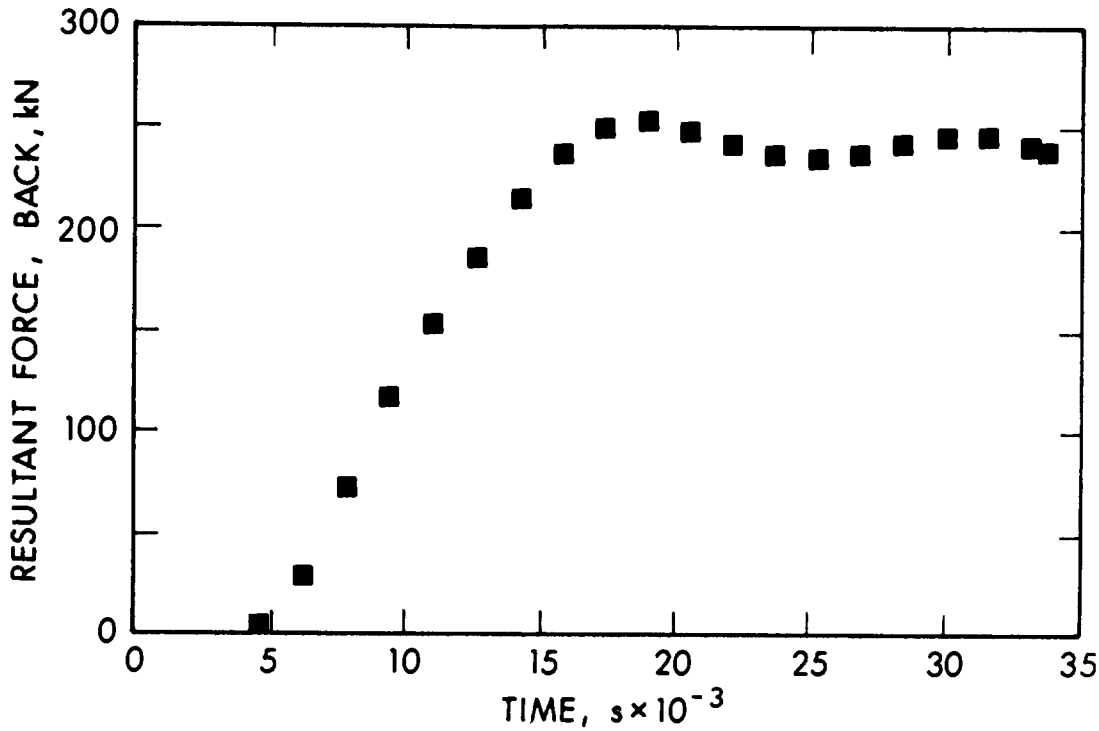

Figure 6a. The resultant force due to overpressure versus time for the back face.

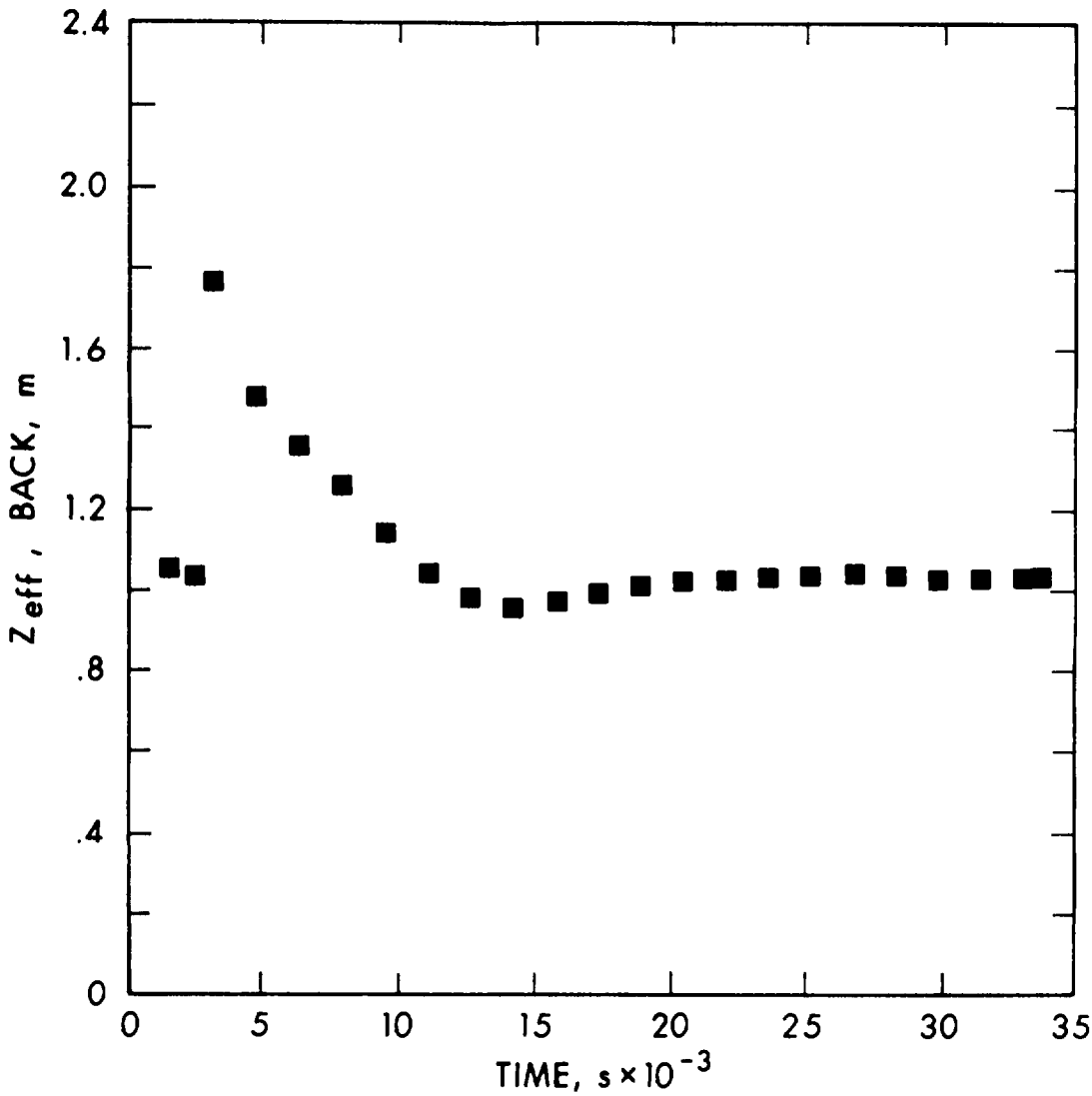

Figure 6b. The Z location of the effective point of application of the resultant force due to overpressure versus time for the back face.

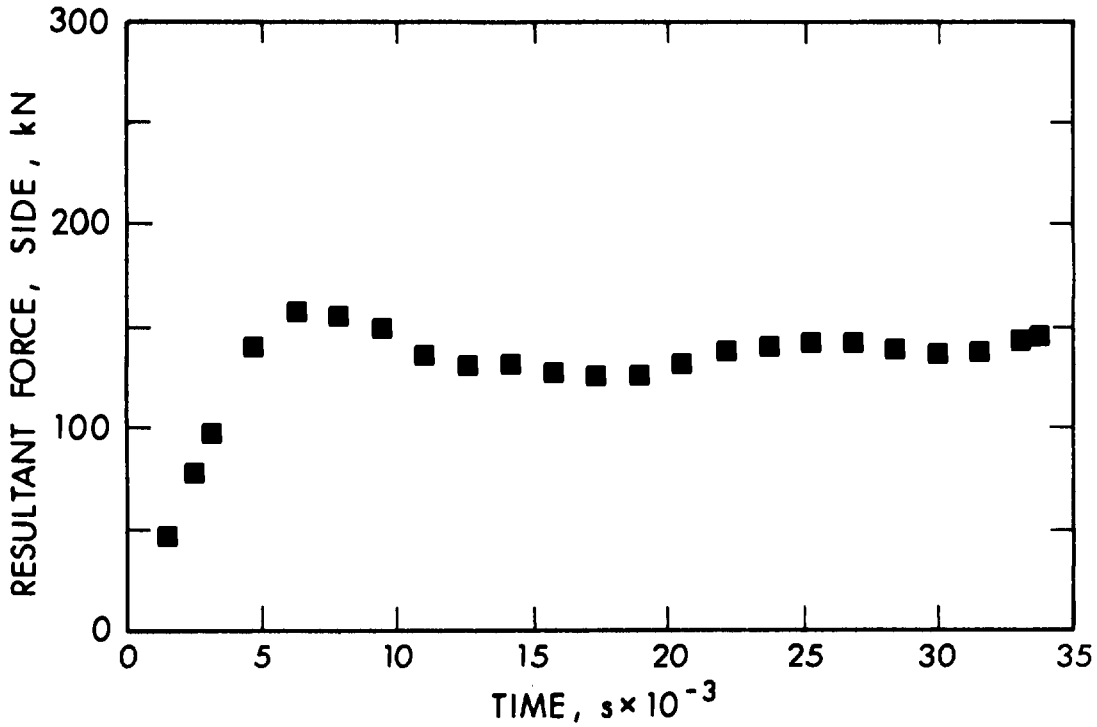

Figure 7a. The resultant force due to overpressure versus time for the side face.

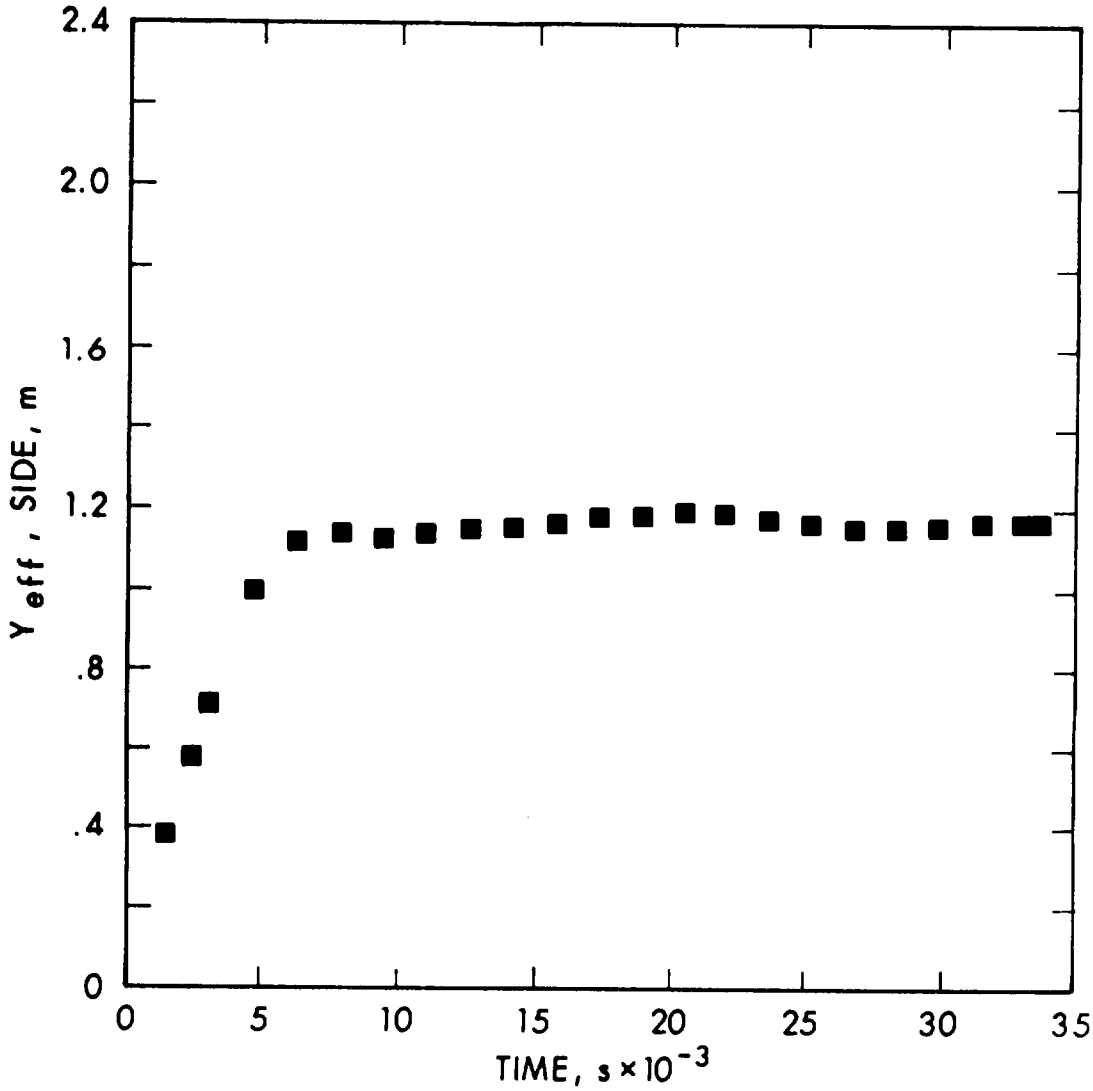

Figure 7b. The Y location of the effective point of application of the resultant force due to overpressure versus time for the side face.

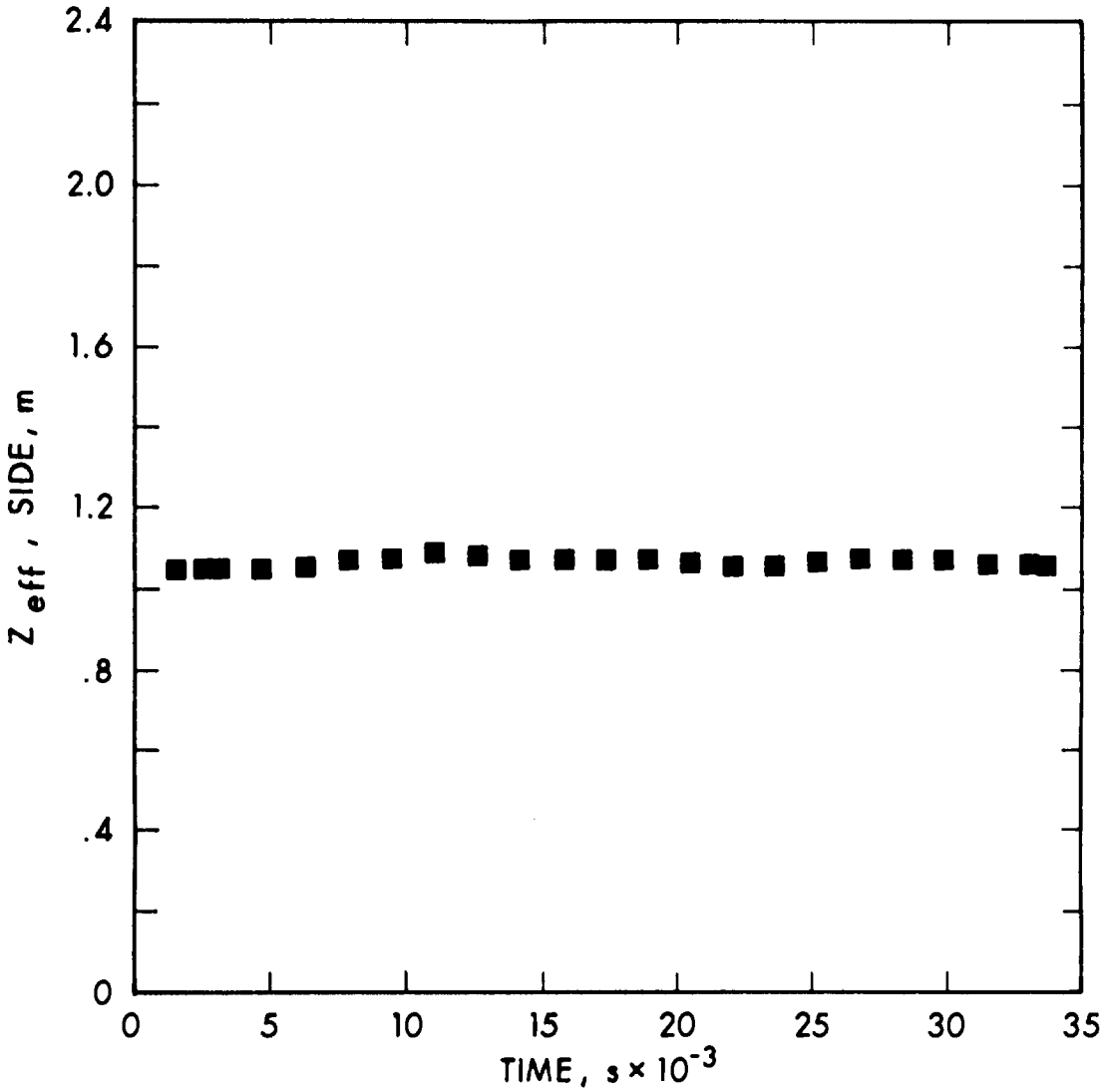

Figure 7c. The Z location of the effective point of application of the resultant force due to overpressure versus time for the side face.

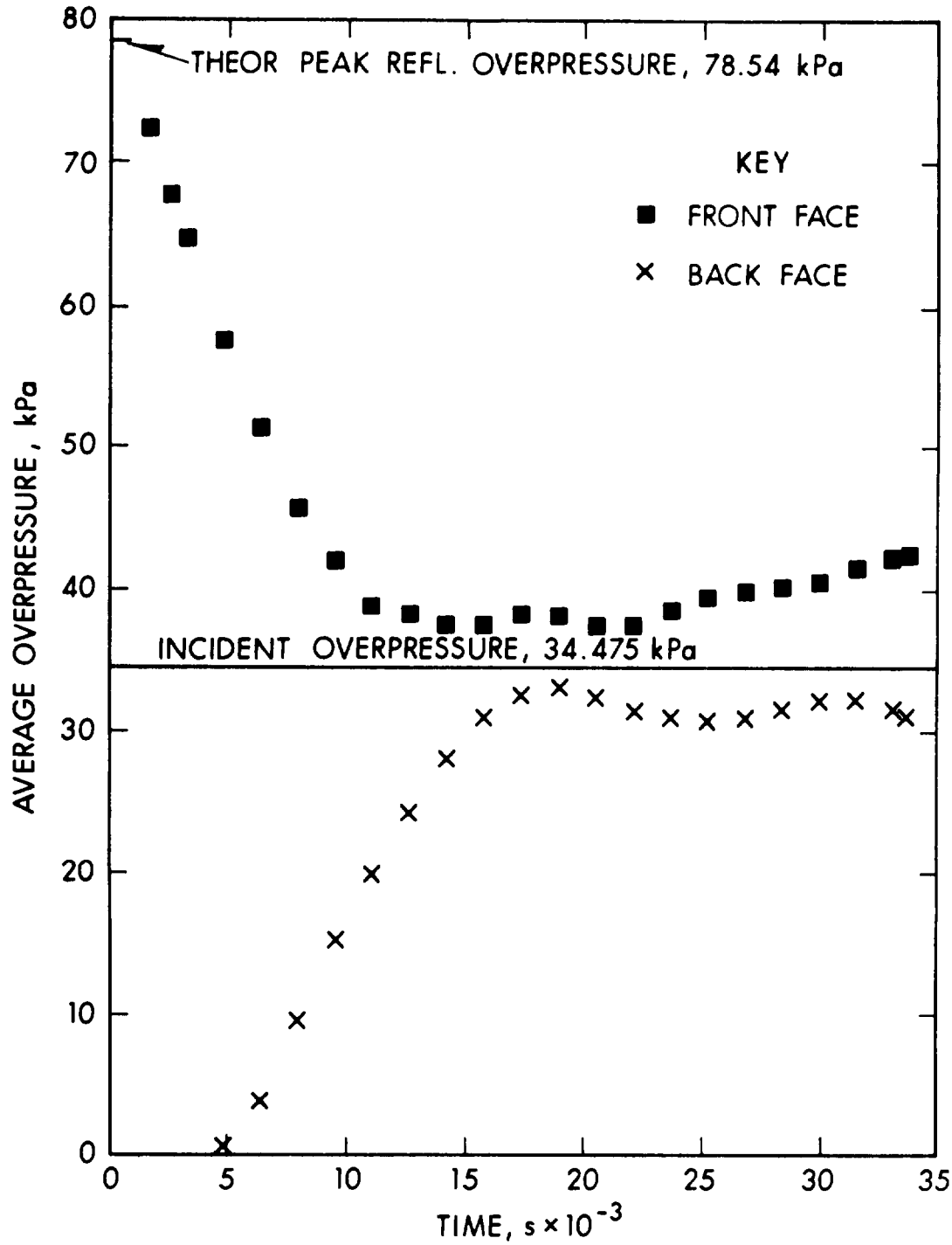

Figure 8a. Comparative plot of average overpressure on the front and back faces versus time.

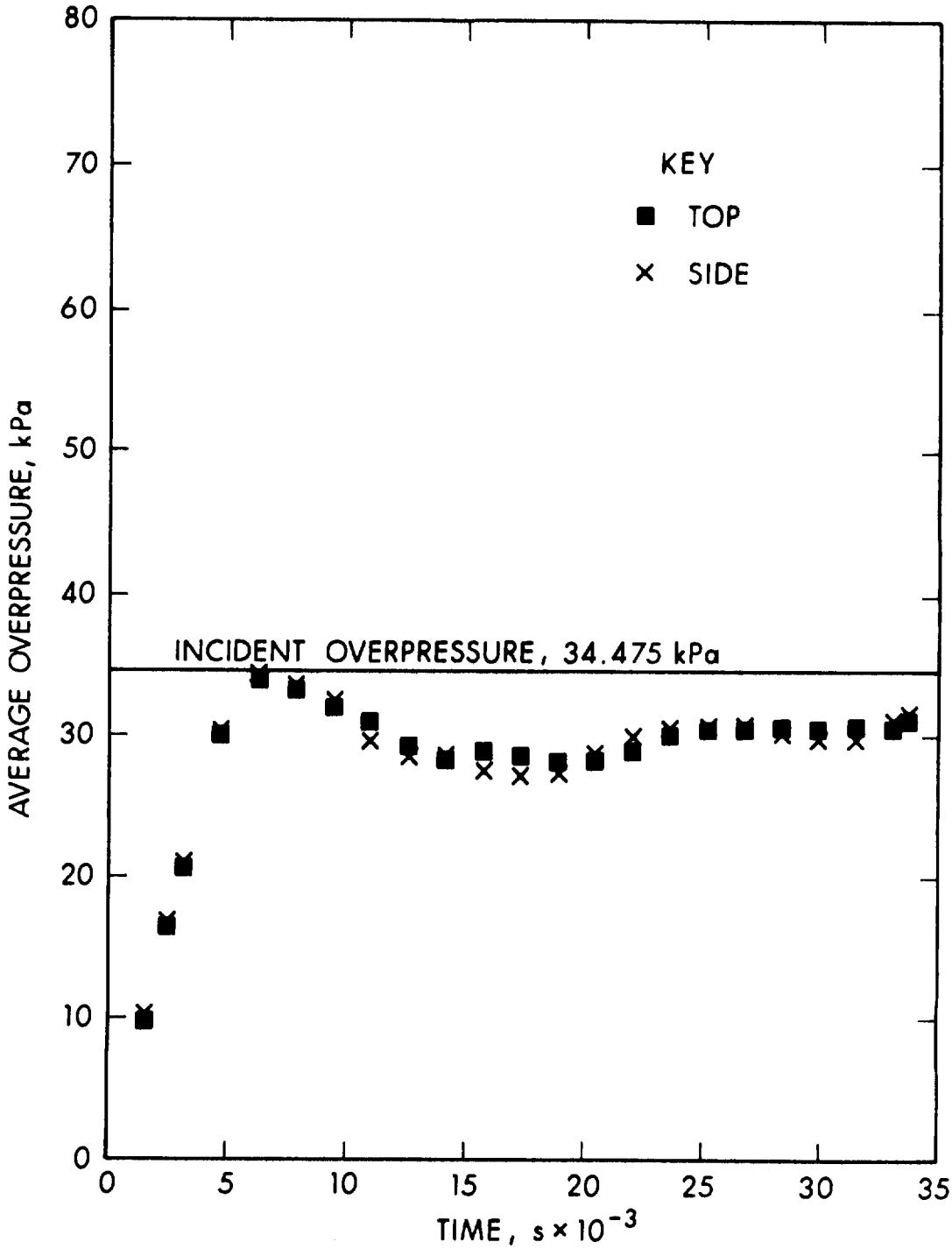

Figure 8b. Comparative plot of average overpressure on the top and side faces versus time.

APPENDIX

A magnetic data tape has been prepared containing the results of the BAAL computation for the shock diffraction loading of a steady, one-dimensional, 34.475 kPa (5.0 psi) overpressure shock wave on an S-280 Electrical Equipment Shelter. Copies of this tape are available upon request. Send tape requests, referring to this document, to:

Director
Ballistic Research Laboratories
Aberdeen Proving Ground, MD 21005
ATTN: AMXBR-TB, Mr. R. E. Lottero

The data tape contains two general sets of information. The first set consists of 102 lines of alphanumeric data describing the numeric data to follow. The alphanumeric data is written so that the tape can serve as a self-contained, clearly interpretable document. When the tape is used as a numeric data source, these 102 lines of alphanumeric data may be skipped, going directly to the first line of numeric data.

The second set of information contains the numeric data, all pertaining to the loading on an S-280 Electrical Equipment Shelter caused by a 34.475 kPa (5.0 psi) steady shock wave. There are cell center overpressures for each flow field cell that has a face coincident with a shelter face for each of 23 points in time. Also included are resultant force due to overpressure for each entire shelter face, and the effective point of application of that force. The 23 points in time represent approximately every fifth computational cycle. The computational time stepping was implicit.

The data is written in a card image format. The tape is 7 track, 800 BPI, even parity, BCD code (IBM 1401), unlabeled, with 80 character lines, and a blocking factor = 1.

DISTRIBUTION LIST

No. of Copies	Organization
12	Commander Defense Documentation Center ATTN: DDC-TCA Cameron Station Alexandria, VA 22314
3	Director Defense Advanced Research Projects Agency ATTN: Tech Lib NMRO PMO 1400 Wilson Boulevard Arlington, VA 22209
4	Director of Defense Research and Engineering ATTN: DD/TWP DD/S&SS DD/T&SS AD/SW Washington, DC 20301
2	Director Weapons Systems Evaluation Gp ATTN: CPT Donald E. McCoy, USN Document Control Washington, DC 20305
1	Director Institute for Defense Analyses ATTN: IDA Librarian, Ruth S. Smith 400 Army-Navy Drive Arlington, VA 22202
2	Asst. to the Secretary of Defense (Atomic Energy) ATTN: Document Control Donald R. Cotter Washington, DC 20301
4	Director Defense Intelligence Agency ATTN: DT-1C/Dr. J. Vorona DI-7D/E.O. Farrell DT-2/Wpns & Sys Div Technical Library Washington, DC 20301
6	Director Defense Nuclear Agency ATTN: SPTD/Mr. J. Kelso SPSS/Dr. E. Sevin SPAS/Mr. J. Moulton STSP STVL/Dr. La Vier RATN/Cdr Alderson Washington, DC 20305
6	Director Defense Nuclear Agency ATTN: DDST/Mr. P. Haas DDST/Mr. M. Atkins STTL/Tech Lib (2 cys) STSI/Archives SPSS/LT J. R. Williams Washington, DC 20305
1	Commander Field Command, DNA ATTN: FCPR Kirtland AFB, NM 87115
1	Chief Las Vegas Liaison Office Field Command TD, DNA ATTN: Document Control P.O. Box 2702 Las Vegas, NV 89104
1	Commander Field Command, DNA Livermore Branch ATTN: FCPRL P.O. Box 808 Livermore, CA 94550

DISTRIBUTION LIST

No. of Copies	Organization
1	Director Defense Communications Agency ATTN: NMCSSC (Code 510) Washington, DC 20305
1	Director Joint Strategic Target Planning Staff JCS ATTN: Sci and Tech Info Lib Offutt AFB Omaha, NB 68113
1	Director National Security Agency ATTN: E. F. Butala, R15 Ft. George G. Meade, MD 20755
1	Commander US Army Materiel Development and Readiness Command ATTN: DRCDMA-ST 5001 Eisenhower Avenue Alexandria, VA 22333
2	Commander US Army Materiel Development and Readiness Command ATTN: DRCRD-WN DRCRD-WN-RE-2 Mr. J. Corrigan 5001 Eisenhower Avenue Alexandria, VA 22333
1	Commander US Army Aviation Systems Command ATTN: DRSAV-E 12th and Spruce Streets St. Louis, MO 63166
1	Director US Army Air Mobility Research and Development Laboratory Ames Research Center Moffett Field, CA 94035
4	Commander US Army Electronics Command ATTN: DRSEL-RD DRSEL-TL-IR R. Freiberg J. Roma A. Sigismondi Fort Monmouth, NJ 07703
1	Commander US Army Missile Command ATTN: DRSMI-R Redstone Arsenal, AL 35809
1	Commander US Army Tank Automotive Logistics Command ATTN: DRSTA-RHFL Warren, MI 48090
2	Commander US Army Mobility Equipment Research & Development Command ATTN: Tech Docu Cen, Bldg 315 DRSME-RZT Fort Belvoir, VA 22060
1	Commander US Army Armament Command ATTN: SARRI-LR/Mr. B. Morris Rock Island, IL 61202
1	Commander US Army Picatinny Arsenal ATTN: SARPA-V Mr. G. Demitrack Dover, NJ 07801
1	Commander US Army White Sands Missile Range ATTN: STEWS-TE-N/Mr. J. Gorman White Sands, NM 88002

DISTRIBUTION LIST

No. of Copies	Organization
1	Commander US Army Rock Island Arsenal Rock Island, IL 61202
1	Commander US Army Watervliet Arsenal Watervliet, NY 12189
6	Commander US Army Harry Diamond Labs ATTN: DRXDO-TI Mr. F. N. Wimenitz Mr. Jim Gaul DRXDO-NP Mr. J. Gwaltney DRXDO-RBH Mr. P. A. Caldwell 2800 Powder Mill Road Adelphi, MD 20783
1	Commander US Army Materials and Mechanics Research Center ATTN: Technical Library Watertown, MA 02172
1	Commander US Army Natick Research and Development Command ATTN: DRXRE/Dr. D. Sieling Natick, MA 01762
1	Commander US Army Foreign Science and Technology Center ATTN: Rsch & Data Branch Federal Office Building 220 7th Street, NE Charlottesville, VA 22901
3	Commander US Army Nuclear Agency ATTN: ATCN-W/CPT M. Bowling CDINS-E Technical Library Fort Bliss, TX 79916
1	Director US Army TRADOC Systems Analysis Activity ATTN: ATAA-SA White Sands Missile Range NM 88002
1	Commander US Army Communication Command ATTN: Technical Library Fort Huachuca, AZ 85613
1	Interservice Nuclear Weapons School ATTN: Technical Library Kirtland AFB, NM 87115
2	HQDA (DAMA-AR; NCB Div) Washington, DC 20310
2	HQDA (DAEN-MC; DAEN-CWE) Washington, DC 20310
2	Department of the Army Office, Chief of Engineers Publications Department ATTN: DAEN-MCE-D DAEN-RDM 890 South Pickett Street Alexandria, VA 22304
3	Director US Army Advanced BMD Technology Center ATTN: CRDABH-X/J. Davidson DRCABH-S/Mr. M. Capps N. J. Hurst Huntsville, AL 35807
1	Commander US Army Research Office P.O. Box 12211 Research Triangle Park NC 27709

DISTRIBUTION LIST

No. of Copies	Organization
4	Commander US Army Engineer Waterways Experiment Station ATTN: Technical Library William Flathau John N. Strange James Ballard P.O. Box 631 Vicksburg, MS 39180
2	Director Defense Civil Preparedness Agency ATTN: Mr. George Sisson/RF-SR Technical Library Washington, DC 20301
1	Commander US Army Engineering Center ATTN: ATSEN-SY-L Fort Belvoir, VA 22060
1	Director US Army Construction Engineering Research Laboratory ATTN: CERL-SL P.O. Box 4005 Champaign, IL 61820
1	Division Engineer US Army Engineering Division ATTN: Docu Cen Ohio River P.O. Box 1159 Cincinnati, OH 45201
1	Division Engineer US Army Engineering Division ATTN: Mr. M. Dembo Huntsville Box 1600 Huntsville, AL 35804
5	Chief of Naval Research ATTN: Code 464/Jacob L. Warner Code 464/Thomas P. Quinn N. Perrone (2 cys) Technical Library Department of the Navy Washington, DC 20360
2	Chief of Naval Operations ATTN: OP-03EG OP-985F Department of the Navy Washington, DC 20350
1	Chief of Naval Material ATTN: MAT 0323 Department of the Navy Arlington, VA 22217
1	Director Strategic Systems Projects Ofc ATTN: NSP-43, Tech Lib Department of the Navy Washington, DC 20360
1	Commander Naval Electronic Systems Command ATTN: PME 117-21A Washington, DC 20360
2	Commander Naval Sea Systems Command ATTN: ORD-91313 Library Code 03511 Department of the Navy Washington, DC 20362
3	Commander US Naval Facilities Engineering Command ATTN: Code 03A Code 04B Technical Library Washington, DC 20360

DISTRIBUTION LIST

No. of Copies	Organization
5	Officer-in-Charge Civil Engineering Laboratory Naval Constr Btn Ctr ATTN: Stan Takahashi R. J. Odello Technical Library Port Hueneme, CA 93041
2	Commander Naval Ship Engineering Center ATTN: Technical Library NSEC 6105G Hyattsville, MD 20782
1	Commander David W. Taylor Naval Ship Research & Development Center ATTN: L42-3 Library Bethesda, MD 20084
2	Commander US Naval Surface Weapons Center ATTN: Code 1224/Navy Nuclear Programs Office Code 730/Tech Lib Silver Spring, MD 20910
1	Commander US Naval Surface Weapons Center ATTN: Technical Library Dahlgren, VA 22448
1	Officer-in-Charge US Naval Weapons Center ATTN: Code P80962 Pasadena Annex 3203 East Foothill Boulevard Pasadena, CA 91107
2	Commander US Naval Ship Research and Development Center Facility Underwater Explosions Research Division ATTN: Code 17/W. W. Murray Technical Library Portsmouth, VA 23709
1	Commander US Naval Weapons Evaluation Facility ATTN: Document Control Kirtland AFB Albuquerque, NM 87117
2	Commander and Director US Naval Civil Engineer Laboratory ATTN: Code L31/Mr. Shaw Mr. R. Siebold Port Hueneme, CA 93041
2	Director US Naval Research Laboratory ATTN: Code 2027/Tech Lib Code 8440/F. Rosenthal Washington, DC 20390
1	Superintendent US Naval Postgraduate School ATTN: Code 2124/Tech Rpts Lib Monterey, CA 93940
1	HQ USAF (INATA) Washington, DC 20330
1	HQ USAF (PRF) Washington, DC 20330
2	AFSC (DLCAW; Tech Lib) Andrews AFB Washington, DC 20331
2	AFATL (ATRD/R. Brandt) Eglin AFB, FL 32542
1	RADC (FMTLD/Docu Lib) Griffiss AFB, NY 13340
1	AFSWC (SWTSX) Kirtland AFB, NM 87117
1	AFWL (SUL) Kirtland AFB, NM 87117

DISTRIBUTION LIST

No. of Copies	Organization
3	AFWL (Robert Port; DEV Jimmie L. Bratton; DEV M. A. Plamondon) Kirtland AFB, NM 87117
1	Commander-in-Chief Strategic Air Command ATTN: NRI-STINFO Lib Offutt AFB, NB 68113
1	AFFDL (FDTR) (Dr. F. J. Janik, Jr.) Wright-Patterson AFB, OH 45433
1	AFML (MAMD/Dr. T. Nicholas) Wright-Patterson AFB, OH 45433
1	FTD (TDPTN) Wright-Patterson AFB, OH 45433
1	AFIT (Lib Bldg 640, Area B) Wright-Patterson AFB, OH 45433
1	Director US Bureau of Mines ATTN: Technical Library Denver Federal Center Denver, CO 80225
1	Director US Bureau of Mines Twin Cities Research Center ATTN: Technical Library P.O. Box 1660 Minneapolis, NM 55111
1	US Energy Research and Development Administration Division of Headquarters Svcs ATTN: Doc Control for Classified Tech Lib Library Branch G-043 Washington, DC 20545
1	US Energy Research and Development Administration Albuquerque Operations Office ATTN: Doc Control for Tech Lib P.O. Box 5400 Albuquerque, NM 87115
1	US Energy Research and Development Administration Nevada Operations Office ATTN: Doc Control for Tech Lib P.O. Box 14100 Las Vegas, NV 89114
2	Director Lawrence Livermore Laboratory ATTN: Larry W. Woodruff, L-125 Technical Information Div P.O. Box 808 Livermore, CA 94550
4	Director Los Alamos Scientific Laboratory ATTN: Doc Control for Rpts Lib R. A. Gentry L. R. Stein C. W. Hirt P.O. Box 1663 Los Alamos, NM 87544
1	Director National Aeronautics and Space Administration Scientific and Technical Information Facility P.O. Box 8757 Baltimore/Washington International Airport, MD 21240
1	National Academy of Sciences ATTN: Mr. D. G. Groves 2101 Constitution Avenue, NW Washington, DC 20418

DISTRIBUTION LIST

No. of Copies	Organization
1	Agbabian Associates ATTN: M. Agbabian 250 North Nash Street El Segundo, CA 90245
2	Applied Theory, Inc. ATTN: John G. Trulio 1010 Westwood Boulevard Los Angeles, CA 90024
1	AVCO Government Products Group ATTN: Res Lib A830, Rm 7201 201 Lowell Street Wilmington, MA 01887
1	The BDM Corporation ATTN: Technical Library 1920 Aline Avenue Vienna, VA 22180
1	Bell Telephone Labs, Inc. ATTN: Tech Rpt Ctr Mountain Avenue Murray Hill, NJ 07971
1	The Boeing Company ATTN: Aerospace Library P.O. Box 3707 Seattle, WA 98124
2	California Research and Technology, Inc. ATTN: Ken Kreyenhagen Technical Library 6269 Variel Avenue Woodland Hills, CA 91364
1	Calspan Corporation ATTN: Technical Library P.O. Box 235 Buffalo, NY 14221
1	Civil/Nuclear Systems Corporation ATTN: Robert Crawford 1200 University, NE Albuquerque, NM 87102
1	EG&G, Incorporated Albuquerque Division ATTN: Technical Library P.O. Box 10218 Albuquerque, NM 87114
1	General American Trans Corporation General American Research Division ATTN: G. L. Neidhardt 7449 N. Natchez Avenue Niles, IL 60648
1	General Electric Company-TEMPO ATTN: DASIAC P.O. Drawer QQ Santa Barbara, CA 93102
1	President General Research Corporation ATTN: Library McLean, VA 22101
1	J. L. Merritt Consulting & Special Engineering Services, Inc. ATTN: Technical Library P.O. Box 1206 Redlands, CA 92373
2	Kaman AviDyne ATTN: Dr. N. P. Hobbs Mr. S. Criscione 83 Second Avenue Northwest Industrial Park Burlington, MA 01803

DISTRIBUTION LIST

No. of Copies	Organization
1	Kaman Sciences Corporation ATTN: Library 1500 Garden of the Gods Road Colorado Springs, CO 80907
2	Lockheed Missiles & Space Co. ATTN: T. Geers D/52-33, Bldg 205 Tech Info Ctr, Doc/Coll. 3251 Hanover Street Palo Alto, CA 94304
1	McDonnell Douglas Corporation ATTN: Robert W. Halprin 5301 Bolsa Avenue Huntington Beach, CA 92647
1	The Mitre Corporation ATTN: Library Rt 62 and Middlesex Turnpike P.O. Box 208 Bedford, MA 01730
2	Physics International Corp. ATTN: E. T. Moore Dennis Orphal 2700 Merced Street San Leandro, CA 94577
4	Physics International Corp. ATTN: Robert Swift Charles Godfrey Larry A. Behrmann Technical Library 2700 Merced Street San Leandro, CA 94577
5	R&D Associates ATTN: Dr. H. L. Brode Dr. Albert L. Latter Bruce Hartenbaum William B. Wright Henry Cooper P.O. Box 9695 Marina del Rey, CA 90291
4	R&D Associates ATTN: Jerry Carpenter Sheldon Schuster J. G. Lewis Technical Library P.O. Box 9695 Marina del Rey, CA 90291
1	Sandia Laboratories ATTN: Doc Control for 3141 Sandia Rpt Collection P.O. Box 5800 Albuquerque, NM 87115
2	Sandia Laboratories Livermore Laboratory ATTN: Doc Control for Tech Lib Doc Control for L. Hill P.O. Box 969 Livermore, CA 94550
1	Science Applications, Inc. ATTN: R. A. Shunk P.O. Box 3507 Albuquerque, NM 87110
3	Science Applications, Inc. ATTN: R. Seebaugh William M. Layson John Mansfield 1651 Old Meadow Road McLean, VA 22101
2	Science Applications, Inc. ATTN: David Bernstein D. E. Maxwell 7850 Edgewater Drive Oakland, CA 94621
2	Science Applications, Inc. ATTN: Technical Library Michael McKay P.O. Box 2351 La Jolla, CA 92038

DISTRIBUTION LIST

No. of Copies	Organization
1	Shock Hydrodynamics, Inc. A Division of Whittaker Corp. ATTN: L. Zernow 15010 Ventura Boulevard Sherman Oaks, CA 91304
5	Systems, Science & Software ATTN: Robert T. Allen Donald R. Grine Ted Cherry Thomas D. Riney Technical Library P.O. Box 1620 La Jolla, CA 92037
2	Terra Tek, Inc. ATTN: Sidney Green Technical Library 420 Wakara Way Salt Lake City, UT 84108
2	Tetra Tech, Inc. ATTN: Li-San Hwang Technical Library 630 North Rosemead Boulevard Pasadena, CA 91107
7	TRW Systems Group ATTN: Paul Lieberman Benjamin Sussholtz Norm Lipner William Rowan Jack Farrell Pravin Bhutta Tech Info Ctr/S-1930 One Space Park Redondo Beach, CA 90278
2	TRW Systems Group ATTN: Mr. F. A. Pieper Greg Hulcher San Bernardino Operations P.O. Box 1310 San Bernardino, CA 92402
2	Union Carbide Corporation Holifield National Laboratory ATTN: Doc Control for Tech Lib Divil Defense Research Prof P.O. Box X Oak Ridge, TN 37830
1	Universal Analytics, Inc. ATTN: E. I. Field 7740 W. Manchester Boulevard Playa Del Rey, CA 90291
1	URS Research Company ATTN: Technical Library 155 Bovet Road San Mateo, CA 94402
1	Weidlinger Assoc. Consulting Engineers ATTN: J. Isenbert 2710 Sand Hill Road Suite 230 Menlo Park, CA 99025
1	Westinghouse Electric Company Marine Division ATTN: W. A. Volz Hendy Avenue Sunnyvale, CA 94008
1	Battelle Memorial Institute ATTN: Technical Library 505 King Avenue Columbus, OH 43201
4	Denver Research Institute University of Denver ATTN: Mr. J. Wisotski Fred P. Vanditti Ron W. Buchanon Technical Library P.O. Box 10127 Denver, CO 80210

DISTRIBUTION LIST

No. of Copies	Organization
3	IIT Research Institute ATTN: Milton R. Johnson R. E. Welch Technical Library 10 West 35th Street Chicago, IL 60616
2	Lovelace Foundation for Medical Education ATTN: Asst Dir of Research Robert K. Jones Technical Library 5200 Gibson Boulevard, SE Albuquerque, NM 87108
1	Massachusetts Institute of Technology Aeroelastic and Structures Research Laboratory ATTN: Dr. E. A. Witmer Cambridge, MA 02139
2	Southwest Research Institute ATTN: Dr. W. E. Baker A. B. Wenzel 8500 Culebra Road San Antonio, TX 78206
4	Stanford Research Institute ATTN: Dr. G. R. Abrahamson Carl Peterson Burt R. Gasten SRI Library, Rm G021 333 Ravenswood Avenue Menlo Park, CA 94025
1	University of California Berkeley Campus, Rm 8 ATTN: G. Sackman 2543 Channing Way Berkeley, CA 94720
1	University of Dayton ATTN: Hallock F. Swift 300 College Park Avenue Dayton, OH 45409
1	University of Illinois Consulting Engineering Services ATTN: Nathan M. Newmark 1114 Civil Engineering Building Urbana, IL 61801
2	The University of New Mexico The Eric H. Wang Civil Engineering Research Facility ATTN: Larry Bickle Neal Baum University Station Box 188 Albuquerque, NM 87131
2	Washington State University Administration Office ATTN: Arthur Miles Hohorf George Duval Pullman, WA 99163
	Aberdeen Proving Ground
	Marine Corps Ln Ofc Dir, USAMSAA ATTN: Dr. J. Sperrazza Mr. R. Norman, WSD